J. Physiol. (1975), **253**, *pp.* 257–301
With 5 plates and 4 text-figures
Printed in Great Britain

AXOPLASM ARCHITECTURE AND PHYSICAL PROPERTIES AS SEEN IN THE *MYXICOLA* GIANT AXON

BY DAVID S. GILBERT

From the M.R.C. Cell Biophysics Unit, Department of Biophysics, King's College, 26–29 Drury Lane, London, W.C.2

(*Received 10 June 1975*)

SUMMARY

1. A technique is described for extracting axoplasm from the giant axon of a marine worm, *Myxicola infundibulum*. The operation can be completed in 10 sec.

2. Axoplasm is pulled from the axon of a living worm as a long, clear cylinder, up to 35 cm long and 70 mg wet weight. The worm regenerates a new giant axon in about 4 months.

3. *Myxicola* axoplasm is a gel, 87% water, held together by protein neurofilaments. It contains small amounts of mitochondria and vesicles, but no detectable microtubules.

4. The internal structure of the gel is superficially similar to that of yarn. Closer inspection with light and electron microscopy, and X-ray diffraction, show it to be organized in a hierarchy of helical forms. Squid giant axons have a similar structure.

5. Initial estimates of the bulk physical properties of extracted *Myxicola* axoplasm give: breaking strength, 1400 g/cm^2; specific gravity, 1·05 g/cm^3; birefringence, $1{\cdot}6 \times 10^{-4}$; index of refraction, 1·351; resistivity, 57 Ω cm. These average values are shown to be compatible with the observed structure and composition.

6. Despite its mechanical strength, the axoplasm gel is so hydrated that Na^+, K^+ and homarine diffuse through it at rates approaching those in free solution. Fewer than about 5% of each of these ions are tightly bound to the gel.

7. It is argued that (*a*) the structure and physical properties of *Myxicola* axoplasm are representative of those in other axons, (*b*) the compound helix architecture results from twist of parallel, cross-linked fibrous proteins, and (*c*) this structure serves as a flexible internal skeleton for nerve cell processes.

INTRODUCTION

In 1843 Remak discovered long, thin, roughly parallel structures, called neurofibrils, in living nerve cells. Later improvements in staining techniques showed them to be distributed throughout the volumes of most nerve cells (Apáthy, 1897; Cajal, 1909). Their distribution and appearance suggested to many observers that they served mechanically, to maintain the elongate shapes of nerve cells (Koltzoff, 1906; von Lenhossék, 1910). Two influential scientists speculated further: Schultz (1871) suggested neurofibrils conduct action potentials; and Apáthy (1897) suggested neurofibrils cross boundaries between nerve cells. The collapse of these two erroneous theories led to loss of interest in these structures. Neurofibrils proved also to be labile, and variable in appearance and so, in many opinions, artifacts (Bayliss, 1914). By default, the supporting and shaping elements of nerve cells were assumed to lie in their outer membranous coverings (Parker, 1929; Weiss, 1964), with help, in some theories, from hydrostatic pressure within the cell (Young, 1944; Cragg, 1955). Now, however, many membranes have been shown to behave like viscous fluids (Singer & Nicolson, 1972; Poo & Cone, 1974), so making these membrane-based architectures less plausible. Here I describe the mechanically robust structure and bulk properties found inside a giant axon. These suggest a return to the earlier idea that nerve cells possess an internal skeleton composed of fibrous proteins.

This initial survey is based on one novel operation, which I discovered in 1969: a rope-like strand of whole axoplasm can be pulled out of the giant axon of a marine fan worm, the polychaete *Myxicola infundibulum*. The operation raised three broad questions, which are of central concern in this paper. (1) Is the operation reliable, with acceptable reproducibility, yield and contamination limits? (2) Is a rope-like strand of axoplasm compatible with the free diffusion of ions, which is required by contemporary theories of action potential propagation? (3) Is the extracted axoplasm representative of that inside this and other axons during life? The answer to each of these questions appears to be yes, but the precision of the data are quite low. The major uncertainties stem from a small, but variable, contamination of the extracted axoplasm, a limited population of accessible *Myxicola* (which precluded use of large amounts of axoplasm), and a scarcity of comparable data from other axons.

The chief new result of the operation is the demonstration of the mechanical strength and integrity of axoplasm from which all enveloping membranes have been removed. The structural basis for this is described in Results, I, and some initial estimates of the bulk properties of axoplasm are given in Results, II. Fresh *Myxicola* axoplasm is shown to be a flexible gel, containing about 4% protein. Most of the protein is in the form of

neurofilaments, which give the gel its strength and integrity. Neurofilaments are apparent only at electron microscope magnifications, but they sometimes aggregate to form the neurofibrils seen by light microscopists (Wuerker & Kirkpatrick, 1972; Gilbert, Newby & Anderton, 1975). *Myxicola's* neurofilament array appears quite orderly at low magnifications, and exhibits an over-all twist, like yarn, together with a microscopic crimp pattern, caused by neurofilaments lying in synchronous, parallel helices. At electron microscope magnifications the roughly longitudinal ordering of the neurofilaments is clear, but no regular lattice is apparent. X-ray diffraction reveals coiled α-helical coils forming the neurofilaments. An hypothesis is presented, to account for the many helical forms found in axoplasm. The hypothesis requires only twist of cross-linked, fibrous proteins.

The following paper gives the chemical composition of *Myxicola* axoplasm (Gilbert, accompanying paper). Preliminary accounts have been published, describing the extraction operation (Gilbert & Shaw, 1969), the light microscopic structure and twist hypothesis (Gilbert, 1972*a*, *b*, 1973), the X-ray diffraction pattern (Day & Gilbert, 1972), and neurofilament morphology and peptide composition (Anderton, Day, Gilbert & Newby, 1974; Gilbert *et al.* 1975). The last study is of interest here because it shows that *Myxicola* neurofilament morphology varies with different treatments, and that the axoplasm contains a Ca-activated protease, which can cleave most neurofilament polypeptides within a few seconds.

Since the seminal papers of Bear, Schmitt & Young (1937*a*, *b*) axoplasm squeezed out piecemeal from squid giant axons has provided most of the available data on axoplasm composition and bulk properties. These data are compared with the corresponding *Myxicola* results in this paper, Several new observations of squid axoplasm structure are also presented here. These were prompted by the *Myxicola* results, and are in close agreement with them, despite known differences in the protein composition of squid and worm axoplasm (Gilbert *et al.* 1975). Neurofilament bundles have also been isolated from axons of mammalian brain (Shelanski, Albert, De Vries & Norton, 1971; Davison & Winslow, 1974), and their proteins partially characterized, though the structure and bulk properties of the bundles are undoubtedly altered by the harsh isolation procedure.

Extraction of *Myxicola* axoplasm appears to be a useful tool in physiological and biochemical investigations, so the operation is carefully documented here. It is much faster (requiring about 10 sec) than extrusion of squid axoplasm (*ca.* 20 min), or isolation of brain neurofilament bundles (*ca.* 3 hr), and consequently *Myxicola* axoplasm should be relatively free from post-mortem changes, such as proteolysis. In contrast, dissection of the intact *Myxicola* axon is more difficult and time-consuming than that of

squid (Binstock & Goldman, 1967). Unlike large squid, *Myxicola* are available in the wild year-round, and will live for up to a year in the laboratory. *Myxicola* can also regenerate their giant axons, a capability never observed in squid. Individual worm and squid axons yield comparable amounts of axoplasm, but the available *Myxicola* population in the U.K. is quite small, therefore squid and brain preparations offer larger total yields.

Like the squid giant axon, the *Myxicola* giant axon is syncytial, that is, formed by the confluence of small axons from many hundreds of nerve cells (Nicol, 1948*a*). Both giant axons also directly innervate the musculature, and mediate the startle reflexes of these animals (Nicol, 1948*b*; Roberts, 1962). The giant axons of earth worms are partitioned by transverse septa, but neither *Myxicola* nor squid axons have such septa. The axon membrane properties, which cause resting and action potentials in *Myxicola*, are very similar to those of squid (Binstock & Goldman, 1967; Goldman & Schauf, 1972; Gilbert & Shaw, 1969).

What does axoplasm do? It is known to serve as a reservoir for inorganic ions, which power the electrical communications along the axon membrane. This function is elucidated here, and in the following paper, with measurements of ion concentrations, ion diffusion coefficients, ion retention by the gel, and axoplasm resistivity. The rapid extraction operation permits simple and direct measurement of these bulk properties; previous estimates usually required major corrections for contributions by surrounding tissues. Axoplasm proteins may also serve in transporting material along axons (Parker, 1929; Ochs, 1972), but this function is poorly understood, and has not yet been studied in *Myxicola*. Finally, the observations of axoplasm structure presented here, together with measurements of protein content and breaking strength, indicate that axoplasm is also specialized to act as a rope-like internal skeleton for the axon.

METHODS

Storage and measurement of worms. *Myxicola* were dug during low tides from estuaries on the south coast of Devon and Cornwall. Worms were stored in a well-lit cold room (5–12° C), and their aerated sea water changed approximately once every month. Worms not damaged during capture will survive these conditions, unfed, for over 6 months. Worms have ranged from 1·3 g (3·5 cm body length when fully contracted), to 10·9 g (7·5 cm), with a median size of approximately 6 g (7·5 cm), when collected. Large worms have been captured throughout the year, suggesting a two year (or longer) life cycle.

Extraction of axoplasm. A short, shallow cut near segment 9, along the ventral mid line of an unanaesthetized, contracted worm, will expose a few clear coils of axoplasm. These may be grasped with forceps and pulled from the worm. The remainder of the axoplasm, both anterior and posterior to the cut, follows through the hole as a long, clear strand (Pl. 1*b*). As axoplasm is extracted the segments of the worm twitch

once sequentially, presumably at the moment the giant axon severs its branches to that segment.

The most useful anatomical landmark for this operation is the dark faecal groove, which runs along the ventral mid line from the tail and swerves to the dorsal side near segment 9. Small, sharp scissors and large, blunt forceps work best; sharp forceps cut through the axoplasm. Solutions containing either Ca ions or high salt concentrations cause the axoplasm to disintegrate, so axoplasm must not come into contact with sea water, or worm guts content, during extraction.

It is much easier to extract the coiled axon of a contracted worm, rather than the extended axon of an elongated worm, so worms should be stimulated to contract before extraction. The weakest link during extraction is where forceps meet axoplasm; this frequently breaks. To reduce tension here, it is useful to tip the worm so that axoplasm is pulled downwards, thus the weight of the strand acts to pull out more axoplasm, rather than to pull against the forceps. With these precautions, the operation is routinely 100 % successful.

Several other dissecting approaches to the *Myxicola* axon have been explored; the one described here is by far the most rapid, and gives the largest average yield, with the least contamination.

Squid giant axons. Several observations concerning *Myxicola* axoplasm were compared directly with axoplasm from giant axons of *Loligo forbesi* and *Loligo vulgaris*, at the Laboratory of the Marine Biological Association, Plymouth, England. Living squid were occasionally available, but most work was based on fibres from the refrigerated mantles of squid caught in a trawl 2 hr or more before dissection.

Although both fresh worm and squid axoplasm usually have similar consistencies, squid axoplasm is much more difficult to extract. The reason for this apparently lies in the differing shapes and branching patterns of the two axons (p. 268), not in the cohesiveness of the axoplasm. Short lengths (1–3 cm) of squid axoplasm can nevertheless be routinely extracted. Longer lengths (5–7 cm) have sometimes been obtained, by cutting into the axon where it enters the mantle, and pulling out the more anterior axoplasm. These lengths of axoplasm have, attached, many of the features of the giant axon in this region, including some small peripheral motor branches, many short fine branches associated with the giant synapse, and stumps of the many branches into which the giant axon divides in the stellate ganglion (Young, 1939). Conventional rolling-out of squid axoplasm (Baker, Hodgkin & Shaw, 1962) is to be preferred for its much higher average yield, when the structure is not required intact.

Microscopy. For light microscopy, blocks of muscle containing the *Myxicola* ventral nerve cord and ventral cuticle were fixed in Bouin's fluid (made with Ca-free artificial sea water), then embedded in paraffin, and stained with haematoxylin and eosin. For electron microscopy, Metuzals' (1969) solutions for fixation and staining were most often used. Samples were fixed for 90 min in 2 % glutaraldehyde (in 70 mM cacodylate buffer, pH 7·2, adjusted to 1015 m-osmole with triple-strength artificial sea water), washed for 15 min in artificial sea water, then post-fixed in a 1·1 % OsO_4 solution with similarly adjusted tonicity and pH, for 30 min to 3 hr. The artificial sea water consisted of (mM): NaCl, 460; KCl, 10·4; $MgCl_2$, 55; $CaCl_2$, 11; $NaHCO_3$, 2·5. Samples floated freely and were not stretched during fixation. Samples were dehydrated in ethanol, cleared in propylene oxide, embedded in Taab Araldite (Ciba), and cut on a Reichert OMU2 microtome. Sections were stained with uranyl acetate and lead citrate (Reynolds, 1963), and examined on a Siemens Elmiskop 1A at 80 kv, or a Phillips 300 at 60 kv. All procedures were carried out near 23° C.

X-ray diffraction. Samples were prepared as follows: freshly extracted axoplasm was rinsed briefly with buffer or stain solution, hung like a clothes line in a desiccator,

and stretched by lead weights (*ca.* 0·25 g) suspended in the middle of each strand. After 2 hr or more, one or two strands of axoplasm were cut into short sticks, and several of these abreast were wedged into a thin-walled glass capillary. The sticks were wetted with water vapour, or with one of several buffers. The capillary was then sealed, and placed in an X-ray beam for 10–80 hr, usually *in vacuo*. CuKα radiation was used, most often from a Hilger-Watts fine-focus X-ray generator operated at 50 kV, and equipped with a toroid camera (resolution approx. 120 Å; Elliott, 1965). Low-angle diffraction was searched for using an Elliott GX3 rotating anode X-ray generator, and either a double-mirror Franks camera (Franks, 1955), or a single mirror coupled to a quartz crystal monochromator.

Water content, specific gravity and refractive index. Water content of axoplasm was measured by drying batches of axoplasm to constant weight at 100° C. The wet batches weighed 102–126 mg, and contained axoplasm from five to six worms. Specific gravity was estimated by briefly immersing fresh axoplasm in one of a range of sucrose solutions, and determining the concentration of sucrose required to give neutral buoyancy. Sucrose solutions contained 20 mM phosphate buffer, pH 7.

The refractive index of axoplasm was measured by laying fresh strands of axoplasm on the prism of a Zeiss Abbe refractometer at 23° C, and illuminating the preparation with a sodium lamp. The refractive index of a solution which mimicked the composition of axoplasm (Gilbert, 1975) was measured in the same way. This solution contained 400 mM glycine, 300 mM-KH_2PO_4, 65 mM nicotinic acid and 3·6 % (w/v) bovine serum albumin.

Retardation. The retardation of axoplasm was measured on a Zeiss polarizing microscope using a quarter-wave plate, a 10/0·22 objective, and the Sénarmont method (Bear *et al.* 1937*a*; Born & Wolf, 1964). Axoplasm diameter was measured using a calibrated micrometer eyepiece; and birefringence was calculated as the ratio of retardation to diameter. The discovery that the Ca chelating agents, EDTA and EGTA (ethylenediaminetetraacetic acid and ethyleneglycol bis-(β-aminoethyl ether) *N*,*N*′-tetraacetic acid), minimized swelling and prevented dispersal of axoplasm in aqueous solutions, greatly aided this part of the analysis. Half molar EDTA, adjusted to pH 7·0 with KOH, was most often used.

Breaking strength. For this measurement a strand of fresh axoplasm was stretched between two paper-covered rods. One rod, attached to a micromanipulator, was slowly hoisted away from the other rod, which was attached to the pan of a balance. The maximum weight supported by the strand was read from the balance, and the strand diameter was measured using an ocular micrometer. Mechanical coupling between axoplasm and rod could be made fairly tight by using absorbent paper, and by coiling the ends of the gel several times around each rod, but this arrangement was not sufficiently tight to permit measurement of stress–strain relationships. Measurements were made in air, and within 1–2 min of extraction, before the gels had dried appreciably.

Resistivity. Axoplasm resistivity (i.e. specific resistance) was measured by connecting a Marconi TF 2000 resistance bridge to axoplasm through bright platinum electrodes. Axoplasm and electrodes were kept in a humid glass chamber near 23° C. The resistance of the electrode-axoplasm interface was also measured and subtracted from the total resistance as follows. Two horizontal platinum plates were positioned on micromanipulators a distance X_1 apart (X_1, *ca.* 1 cm). A strand of axoplasm several centimetres long was stretched taut across the air gap, X_1, and the ends were laid on the platinum plates. The plates were connected to the resistance bridge, and the resistance, R_1, of this configuration was measured. The average diameter, D, of the axoplasm in the air gap was measured with an eyepiece micrometer, then the platinum plates were moved together so that the axoplasm hung in a

U-shape between them. Motion of the plates continued until the U fully closed. The resistance, R_2, of this configuration was measured, as was the new distance, X_2, between the plates (X_2, *ca.* 0·5 mm). In practice, R_2 was about one tenth the size of R_1. Resistivity, ρ_A, of the axoplasm in the air gap was calculated from the formula:

$$\rho_A = \frac{\pi}{4} D^2 \left[\frac{R_1 - R_2}{X_1 - X_2}\right]. \quad (1)$$

Diffusion and binding of Na^+, K^+ and homarine. Diffusion of ^{22}Na radially out of axoplasm was measured by incubating, for 1 hr, a strand of freshly extracted axoplasm in 0·5 ml. buffer with 2μCi added ^{22}Na (as $^{22}NaCl$, Amersham Radiochemical Centre). The buffer contained 150 mM-K_2SO_4, 10 mM-Na_2SO_4, 30 mM phosphate, pH 7·2, and was adjusted to 1050 m-osmole with sucrose. The mean diameter and length of the strand were measured; it was then tied to the arm of a stirring motor, and stirred, first in a rinse (100 ml. of the same buffer), then in twenty successive tubes each containing 8 ml. of the same buffer, for 30 sec each, at 18° C. The axoplasm, and all tubes, were counted in a Panax shielded counter, to determine the time course of ^{22}Na efflux from the strand.

The diffusion equation, applied to radial diffusion out of an infinite, homogeneous cylinder of radius a, into an infinite, well-stirred medium, specifies that $S(t)$, the average Na content of the cylinder at time t is:

$$S(t) = (\text{const}) \sum_{n=1}^{\infty} \alpha_n^{-2} \exp(-D_r \alpha_n^2 t),$$

where α_n is the nth root of $J_0(\alpha a) = 0$ (Carslaw & Jaeger, 1959). All data were well fitted by a single exponential, so a negligible error is introduced by dropping all but the first term in this rapidly converging series. Therefore D_r, the radial diffusion coefficient is

$$D_r = (\tau \alpha_1^2)^{-1}, \quad (2)$$

where τ is the time constant of the Na efflux, and $(a\alpha_1) = 2{\cdot}4048$. Efflux time constants in all experiments were determined from regression lines of ln (S) on time. Correlation coefficients are given as measures of goodness of fit.

Longitudinal diffusion of ^{22}Na was measured by draping a strand of axoplasm through an air gap between two small (1 ml.), level, unstirred pots. The 'cold' pot contained 1 ml. 0·5 M-Na_2SO_4, 30 mM phosphate buffer, pH 7·0; the 'hot' pot contained the same solution plus 1μCi ^{22}Na. The total amount of ^{22}Na which diffused along the strand and into the cold pot was measured as before. The longitudinal diffusion coefficient, D_L, was calculated as:

$$D_L = \frac{Jx}{CAt}, \quad (3)$$

where J is the number of counts reaching the cold pot in time t (2·6–18·2 hr); x is the length of axoplasm between pots (3·9–6·0 mm); A is the mean cross-section area of axoplasm over the length x (0·08–0·11 mm^2); and C is the mean difference in activities (counts/cm^3) of the two solutions. Temperature was (18·4 ± 1·6) °C.

Attempts to corroborate the diffusion coefficient measurements with direct measurements of Na^+ and K^+ activities in axoplasm, by means of large, ion-selective glass electrodes (E.I.L. Type GKN 33B and GEA 33B) pressed against fresh axoplasm, gave erratic results under all conditions tested, and so were discontinued. Effluxes of native Na^+ and K^+ from five pooled gels (144 mg, 24° C), into 10 ml. aliquots of isosmotic sucrose, were measured by flame photometry (Gilbert, 1975). Axoplasm was stirred for approximately 1 min in each of seven aliquots, then transferred with forceps to the next.

Upper limits for bound Na^+ and K^+ concentrations were initially estimated in the next experiment by stirring three strands (52 mg, 22° C) in 50 ml. of isosmotic sucrose, pH 6·0, for 33 min, then withdrawing the axoplasm crushing it in dilute HNO_3 and measuring Na^+ and K^+ concentrations of sucrose and axoplasm by flame photometry. These, and the following values, are upper limits for the amounts of cations bound, since electroneutrality requires some cations be retained in the gel, and so appear to be bound in these experiments, although they may, in fact, be freely exchangeable.

Diffusion in a more physiological environment was measured by taking advantage of an intensely U.V.-absorbing constituent of *Myxicola* axoplasm, tentatively identified as homarine (mol. wt. 137; Gilbert, 1975). Strands of fresh axoplasm were stirred in five aliquots (3 ml. each) of an 'artificial axoplasm' containing 250 mM-K_2SO_4, 10 mM-EGTA, 10 mM-KH_2PO_4, and adjusted to pH 7·3 with KOH. Ultraviolet absorption of all solutions was measured at 272 nm.

Finally, more exact estimates of the upper limits for the amounts of Na^+, K^+ and homarine bound in axoplasm were made by gently stirring three strands of axoplasm, initially 56–81 mg, in 50 ml. distilled water (25° C). Samples of solution were taken 3–5 min, and 30 min after immersion, and the axoplasm was then homogenized in a small, measured volume of the same solution with added, dilute H_2SO_4. Samples, axoplasm homogenates, and similarly treated blanks were then assayed for Na^+, K^+ and homarine as before.

All repeated measurements are given as mean ± S.D. of an observation.

RESULTS

I. Structure

Axoplasm geometry; gel and segmental helices

Axoplasm comes out of the worm as a long, clear, elastic, and roughly cylindrical gel (Text-fig. 1 and Pl. 1*B*). Axoplasm from the region near the 15th segment has the maximum diameter, typically near 500 μm; this diminishes approximately linearly with distance towards the tail. The length of extracted axoplasm, about 20–30 cm, is close to that of the fully extended worm. There are two periodic distortions of the extracted gel cylinder: first, the axis of the cylinder is curved into a shallow, right-handed helix, with a pitch of a few millimetres; secondly, in each gyre of this helix, the axoplasm is locally flattened, giving it an elliptical cross-section.

The source of these distortions was investigated by dissecting worms fixed in Bouin's fluid. Worms fixed when stretched had similar distortions of their giant axons, indicating that the distortions were not artifacts of the extraction operation. Worms fixed in a contracted state show how these distortions arise: when the worm contracts, the giant axon is thrown into one large coil in each segment of the worm (Text-fig. 1). The coils are separated by short, straight regions, which are tightly corseted by the connective tissues of the intersegmental septa. These coils of the axoplasm gel approximate a right-handed helix, which I have called the 'gel helix' (Gilbert, 1972*b*), to distinguish it from four smaller helical structures described later. The stretched-out remnants of the gel helix apparently give rise to the shallow coiling of extracted axoplasm.

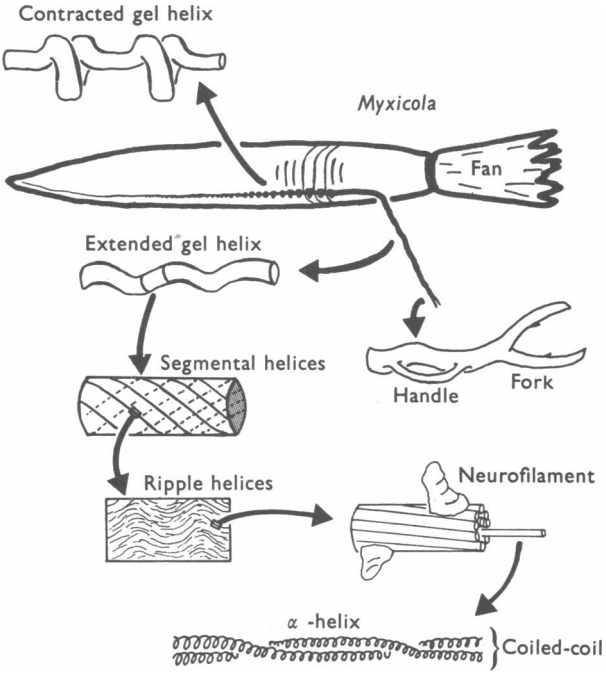

Text-fig. 1. Schematic diagram of extraction and structure of *Myxicola* axoplasm. The giant axon runs the length of the worm inside the ventral nerve cord, and has many hundreds of small branches, often with cell bodies attached, distributed along its length, but omitted here for clarity. The giant axon is approximately cylindrical, and tapers towards either end. As the worm extends and contracts, so do the coils of the giant axon (called here the gel helix, pitch about 2 mm). The extended coils have an internal structure resembling yarn, in which neurofilaments run helically down the gel (the segmental helices, pitch about 2 mm). But as they go, the neurofilaments also show microscopic, synchronous waves (the ripple helices, pitch about 10 μm). A speculative neurofilament structure is also drawn: electron microscopy shows these have lengths often in excess of 10 μm, a backbone diameter near 70 Å, and side arms of variable shape (Gilbert *et al.* 1975). X-ray diffraction indicates that α-helical coiled-coils run down the neurofilament backbone.

The elliptical distortion also arises in these coils, for the axoplasm, like most cylindrical elastic solids, takes on an elliptical cross-section when tightly coiled. Both distortions become smoothed out as the gel swells slightly in most buffer solutions.

The gel helix coils are so tight in a contracted worm that the axon and sheath membranes do not appear to penetrate to the inside of the coil, in light and electron microscope sections. Some regions of the membrane must therefore slide over portions of the axoplasm during the worm's contraction, in order to escape from the coil. In sections, the axon simply seems to widen in each segment. Nicol's (1948*a*) suggestion, that this appearance is due to a sudden liquefaction of all the axoplasm in each bulge, cannot be easily reconciled with the observed gel helix coils, or with

the fact that axoplasm can be extracted. Since vertebrate axons form superficially similar bulges (Cajal, 1928, p. 647; Young, 1944; Weiss & Hiscoe, 1948; Parker, 1929), this type of coiling may be of widespread occurrence.

A second helical form may be seen by tearing fragments from axoplasm. As in geological assays, cleavage indicates the directions of strongest and weakest bonding. Axoplasm cleaves spirally, like yarn. When a small portion of the axoplasm is grasped with fine forceps and pulled, a long, narrow fragment tears away along a right-handed helical path, down the surface of the extended gel helix (Text-fig. 1). These paths I have called 'segmental hèlices' (Gilbert, 1972*b*), because they rotate through approximately one turn within each segment of the worm. They are demonstrable in both extracted axoplasm, and in axoplasm dissected from fixed, stretched worms. Polarizing and electron microscope observations, given later, show that these helices are the directions of strongest bonding because most neurofilaments are aligned along them. Thus the gross internal structure of extended axoplasm resembles that of a single strand of yarn: the fibres of the yarn are the neurofilaments; the twist of the yarn gives the segmental helix paths seen during cleavage; and the entire array forms a closely packed, flexible cylinder.

The limitations of this assay and slight departures from the yarn model given above are noted here because cleavage studies furnish more information about the long-range paths of neurofilaments than any of the microscopic methods in this paper. This is a consequence of a neurofilament's small diameter, great length and non-planar path, all of which make their pursuit through thin sections very difficult. The chief limitations of cleavage studies are: (*a*) diffuse, small or weak structures cannot be detected; (*b*) plastic deformations render the assay qualitative rather than quantitative; (*c*) structures near the centre of the axoplasm are difficult to assay; (*d*) and neurofilaments might systematically cross directions of cleavage, though this has not been detected, and is assumed not to occur. Some non-uniform twist within axoplasm, perhaps about more than one axis, thus cannot be entirely ruled out. The main departures from a uniform yarn structure appear to be these: (*a*) the pitch angles of the segmental helices vary within each segment. This is related to the elliptical distortion of the gel (see Gilbert, 1972*b*, fig. 4). (*b*) Fragments tend to dive slightly towards the centre of the gel. (*c*) The taper of the axoplasm, and the shorter segment lengths towards the tail of the worm, require modification of the yarn model. Polarizing microscopy (Gilbert, 1972*b*, fig. 7) indicates that both may be accounted for simply by making twist (number of turns per unit length) inversely proportional to axoplasm diameter.

The relationship between gel and segmental helices is also most simply understood by considering axoplasm as a single strand of yarn: when the ends of a short strand of yarn are moved together, the yarn forms a coil (the gel helix), and when the ends are moved apart, twist is conserved, and exhibits itself in the segmental helices. As nearly as I can determine, both configurations in axoplasm reflect the same amount of twist, one turn per segment.

Does axoplasm actively coil itself? Axoplasm can be made to twist actively (p. 291), and therefore might do so during contractions of the worm. However, the observed, but approximate, conservation of twist indicates that axoplasm behaves like a passive, elastic spring during formation of the gel helix coils. Also, extracted axoplasm has never shown rapid spontaneous movements of any but a purely elastic type.

Axoplasm from squid axons also has a right-handed segmental helix twist (Metuzals & Izzard, 1969; Gilbert, 1972*b*), even though squid giant axons do not normally form gel helix coils. Twist of filaments in smaller axons has occasionally been noted (Wuerker & Kirkpatrick, 1972; Weiss & Mayr, 1971*b*, fig. 3), but not explored.

Branches

So cohesive is axoplasm that some of the larger branches of the *Myxicola* axon are visible as membrane-free branches emanating from the extracted axoplasm. In setiger 2, for example, the giant axon forks into two branches of nearly equal diameters; these circle the oesophagus, taper, and terminate in the supra-oesophageal ganglia (Nicol, 1948*a*). Axoplasm extracted from these segments usually shows a closely corresponding fork, and tapering branches, with dimensions similar to those found *in situ* (Text-fig. 1, and Gilbert, 1972*b*, figs. 2 and 8).

Other large branches visible on extracted axoplasm arise from the 'handles' of the giant axon. These are large branches which merge back into the giant axon only one segment away from their origin (Nicol, 1948*a*), so resembling the handle of a teacup. My dissections indicate one handle spanning each intersegmental septum from setiger 2 to about setiger 12. The arrangement of handles varies: a handle on the right side of the giant axon is usually, but not always, followed by a handle on the left, and, infrequently, the handle diameter may rival the axon diameter. The more posterior handles have diminishing diameters, so handles posterior to setiger 12 may have been overlooked. Handles appear frequently on axoplasm extracted from the first few segments, though they are usually broken at one end during extraction by the tough connective tissues of the septa.

The handles often have visible membranous contaminants attached after extraction, so axoplasm from the anterior segments was discarded before contaminant-sensitive analyses. The large handles also dictated the choice of setiger 9 as the site of extraction, since these handles make extraction from the more anterior segments risky. Fragments torn from the larger handles or anterior forks leave helical scars around these processes, indicating that these have structures much like that of the main trunk. Scars at the crotch regions point to a structure similar to the division of the axon model in Pl. 5*C*, except that a small minority of filaments probably runs directly from one daughter branch to the other, since these regions are, initially, relatively difficult to split.

Processes of the giant axon smaller than about 50 μm in diameter (branches, handles, etc.) are not visible on the extracted axoplasm, and so

must have been either broken off in place, or dissolved away by extracellular fluids during extraction. Nicol (1948*a*) noted that most peripheral branches of the giant axon are very small, only 2–10 μm in diameter. Some of these finer processes may be seen by fixing the entire ventral cord in glutaraldehyde (formaldehyde leaves the axoplasm too brittle), and then extracting the fixed axoplasm, in the manner described for fresh axoplasm. This procedure gives a fine cast of the entire axon, including the stumps of the few larger branches (up to 70 μm diameter), and long lengths of some of the smaller branches, both bristling from the ventro-lateral surfaces of the coils of the giant axon.

This fine cast of the giant axon illustrates two probable causes for the success of the extraction operation: first, the cross-sectional area of the giant axon, through which the extracting forces are transmitted, is very large compared to the local sum of the branch cross-sectional areas, through which most of the opposing forces are transmitted. Secondly, the coiling of the giant axon into the gel helix allows the branches of only one segment at a time to take the entire strain, so they are broken segment by segment. This observation helps to explain the increased difficulty met in extracting axoplasm from a worm which is not contracted, and from squid giant axons, which are not coiled.

Contamination

Extracted axoplasm is normally transparent and colourless. Infrequently there is visible contamination, which may arise from one of several sources. Fortunately, some of these are colour-coded: a pale-green strand of axoplasm indicates that one of the blood vessels has been punctured. Milky-white strands arise from contamination by gonadal material. Orange strands show that attached musculature has been pulled out. Whitish corsets correspond to portions of the ventral cord sheath. Thinner, transparent patches of membrane show up between crossed polarizers; they are probably axon sheath material. These last patches cover a few percent of the surface area of typical strands. Contaminants are most frequently evident in the region grasped by forceps, so this region was customarily cut off and discarded when high purity was required. Outside this region the unaided eye can pick out coloured contaminants on approximately one in ten strands, so permitting simple control of purity. Contamination by less densely coloured material is a difficult and unresolved issue. It is discussed with electron microscopy, and with resistivity. The Na concentration in extracted axoplasm appears to be a sensitive, and easily measured indicator of contamination (Gilbert, 1975).

Yield

Text-fig. 2 shows the yield of axoplasm obtained from worms of various sizes. Part of the scatter is due to the strand breaking before extraction was completed, but much of it is due to genuine variation of axon size with worm weight, as noted by Nicol (1948*a*). Storage of worms for a month or more causes appreciable loss of body weight without greatly affecting the weight of axoplasm (Fig. 2).

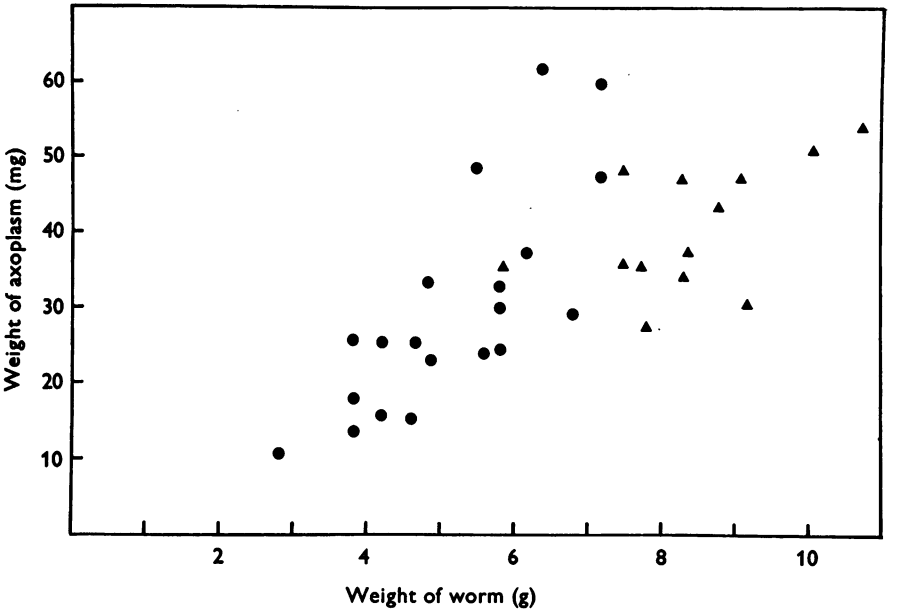

Text-fig. 2. Axoplasm weight plotted against the weight of the worm from which it was extracted. (●) represents worms stored for approximately one month before extraction; (▲) represents worms stored for 1 day before extraction. Two trends emerge: The larger the worm, the larger its axon; and, long storage leads to marked loss of body weight, but little loss of axoplasm weight.

Axoplasm from, for example, a 7·3 g worm, was 28 cm long (unstretched), and weighed 47 mg. Its maximum diameter was 970 μm; this dwindled to 170 μm at the tail end, and to about 80 μm at the tips of the anterior forks. Its largest handle was torn at the anterior end, and measured 150 μm in diameter.

Light microscopy

Freshly extracted axoplasm in 0·5 M-EDTA, pH 7·0, or liquid paraffin, is striking for its transparency and homogeneity, when examined using bright-field or phase-contrast microscopy. In dark-field, it scatters light weakly. The chief inhomogeneity in these preparations consists of small,

refractile globules dispersed throughout the gel, which, with time (about 30 min) apparently coalesce into larger refractile globules, some tens of microns in diameter. Infrequently, a row of highly scattering inclusions is visible near the centreline of the gel. These resemble the 'massive bodies' commonly found in squid giant axons, which, according to Villegas (1969), consist of dense aggregations of vesicles.

Sections of fixed nerve cords show that extraction removes nearly all the axoplasm from the giant axon (Pl. 1*C*). The neuropil swells upward to fill partially the hole left by the axon; this leaves a crescent-shaped gap, bordered ventrally by a fine filigree of ventral cord tissue. The gap contains some debris, but little, if any, residual giant axoplasm, as judged by its light, even staining, and slight birefringence.

Polarizing microscopy. Extracted axoplasm is positively birefringent, that is, its refractive index is larger in the longitudinal than in the radial direction. This arises from its refractile fibrous proteins, which are preferentially oriented in the longitudinal direction (see Electron microscopy). The protein orientation, and hence the birefringence, varies slightly from place to place in axoplasm. There are both macroscopic and microscopic variations. Macroscopically, birefringence varies most along the radius of the axoplasm, and, microscopically, there is a complex ripple pattern (Pl. 3*A*).

Preliminary macroscopic observations showed that two factors affect the magnitude of the measured birefringence: strain, and bathing medium. Axoplasm stretched to near the breaking point will increase its birefringence at least twofold. This effect has not been explored quantitatively, because of the difficulty in mechanically coupling to the gel. Bathing media may disperse axoplasm (Gilbert, 1975), causing the birefringence to disappear at about the same rate as the structural integrity of the gel. Alternatively, if the medium is aqueous, close to isosmotic, and near pH 7, the gel usually swells, and its birefringence decreases. A typical peak value for the birefringence of unstressed axoplasm is $1{\cdot}6 \times 10^{-4}$, when measured in liquid paraffin. In buffered, 0·98 m sucrose (which has the same osmolarity as axoplasm, but in which the gel swells), peak birefringence is about 3×10^{-5} (Text-fig. 3). In these and the following measurements a visual average was taken over several periods of the microscopic ripple pattern. Squid axoplasm, which has a very different protein composition (Gilbert *et al.* 1975), has a similar birefringence, $1{\cdot}5 \times 10^{-4}$ (Bear *et al.* 1937*a*) as does frog sciatic axoplasm ($2{\cdot}4 \times 10^{-4}$, Thornberg & De Robertis, 1956). Resolution of birefringence into form and intrinsic components, as done by these authors, was not attempted, because this requires fixing the axoplasm proteins. Fixation often causes neurofilaments to aggregate, thus one risks creating the very aggregates one seeks to measure.

Retardation varies from place to place across the diameters of both extracted worm and squid axoplasm, as shown in Text-fig. 3, but is roughly constant along any line parallel to the edge of the gel. The double-peaked curve is typical, although infrequently such curves exhibit only a single, central peak. The double peak could arise from a central core of axoplasm having a lower number of filaments per unit volume, or a lower percentage of longitudinally oriented filaments. Both of these

factors are said to occur in squid axoplasm (Metuzals & Izzard, 1969), and both are consistent with axoplasm being shaped by the torques of its filaments (Gilbert, 1972*b*). Electron micrographs of both intact and extracted *Myxicola* axoplasm show greater longitudinal ordering in the periphery, but I have not tested for a difference, in the number of filaments per unit volume, between the periphery and centre of the gel.

A third factor contributing to the central dip in the retardance curve (Text-fig. 3) is that neurofilaments course helically up the gel, at angles up to about 15° to the gel axis. A calculation performed on a Poincaré sphere (Shurcliff & Ballard, 1964) shows that this twist will cause a dip of less than 10 % of the peak value in the retardance *vs.* diameter plot, indicating that the segmental helix twist is not the primary cause of the dip in the curve.

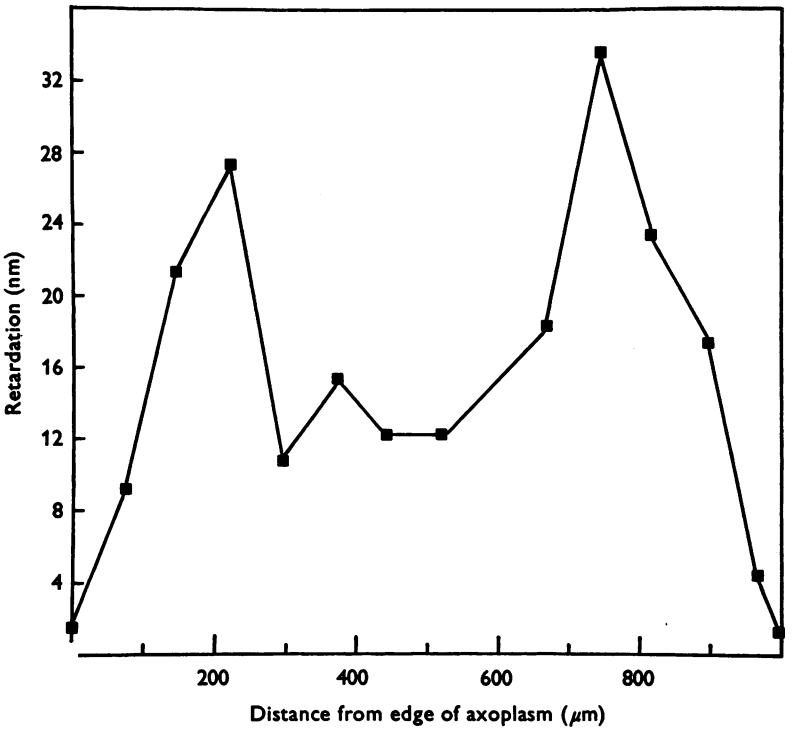

Text-fig. 3. Retardation measured at several positions across the diameter of a 1000 μm strand of extracted *Myxicola* axoplasm, oriented at 45° to crossed polarizers. Axoplasm was swollen, but not stretched. Medium: 0·98 molal sucrose, 20 mM phosphate, pH 7·0.

Ripple. Myxicola axoplasm has a striking array of transverse light and dark bands, when viewed in a polarizing microscope (Pl. 3*A*). Squid axoplasm has a similar array (Pl. 3*B*). I have called this array 'ripple' because of its similarity to the regular progression of small waves in water. Unlike true waves, however, the pattern is unchanged by the passage of time or

even by fixation. Nor is it the frozen path of a primitive wave, which, for example, left refractile material in regularly spaced rows. The refractile material, rather, is uniformly distributed, but varying in orientation. This can be shown by rotating the axoplasm just through the extinction position in a polarizing microscope; this motion converts a dark band at any point in the gel into a light band at the same point. Thus the dark bands represent, not the absence of material, but material oriented near the extinction direction.

Stretching the axoplasm causes the ripple pattern to disappear, but it reappears on release. This observation, together with the positive sign of the birefringence, indicate that ripple arises from a stable, spatially synchronized folding of the fibrous proteins as they course down the axon. Intensity of the ripple varies approximately sinusoidally with distance, so I initially assumed that the fibrous proteins oscillated in sine waves down the axon. Since sine waves are planar, there should be one orientation in which they show no ripple, but I could not find such an orientation in fragments torn from the gel. This indicated that the folding is three-dimensional. The simplest repetitive, three-dimensional folding is a helix. Parallel helices of the same dimensions can pack tightly together, giving spatially coherent 'waves' over long distances in all three dimensions of space, just as is seen in the ripple pattern. This spatial coherence, and the spring-like elastic recovery of the ripple pattern after many cycles of stretch and release, suggested that ripple arose from fibrous proteins packed into locally parallel, 'paranemic' (John & Lewis, 1965) helices, called here the 'ripple' helices.

The most direct evidence linking ripple with a helical configuration is discussed under electron microscopy. Some indirect evidence favouring this hypothesis was obtained by rotating gel fragments in a polarizing microscope (Gilbert, 1972*b*), though distortions introduced during sample preparation made this difficult and often equivocal. These also indicated that ripple helices are right-handed; though twisted-filament models (see Discussion) point to a left-handed ripple helix. Ripple handedness thus remains unresolved. Optical diffraction from the ripple in whole axoplasm was too weak to be visible using laser (3 mW, 632 nm) irradiation. Nomarksi interference contrast views of both fresh axoplasm, and glutaraldehyde-fixed, epon-embedded sections, though showing ripple more faintly, corroborated the polarized light observations.

Ripple wave-length is not uniform across the diameter of the gel, as shown in Pl. 3*A*. This distribution is difficult to study in whole axoplasm because patterns generated at different depths of the gel overlap in the image, since an out-of-focus sine wave grating closely resembles an in-focus one. The least ambiguous results have come from extracted axoplasm, fixed and embedded as for electron microscopy (to prevent distortion), but cut into sections 6 μm thick. Ripple is difficult to see in thinner sections; whereas thicker sections are more difficult to cut and to flatten. These sections show a central and dominant ripple wave-length of about 10 μm, running throughout the length of the gel, and usually flanked by regions of longer and shorter wave-lengths (Pl. 3*A*). The cause of these variations in ripple wave-length is not understood (they may perhaps arise from the straightening of the gel helix, which must stretch different regions within the gel to different extents), nor have the variations been thoroughly mapped, due to difficulties with serial sectioning at this thickness. Optical diffraction of photographs of ripple indicates a wide scatter of periodicities about a mean near 10 μm. The ripple wave-length distribution is also complicated by the segmental helix, and by oblique lines of stress across the bulges,

and so has not been analysed in greater detail. In whole axoplasm the ripple distribution often gives the impression of a wide pipe (*ca.* $\frac{1}{3}$–$\frac{1}{2}$ the gel diameter), with bright corrugated walls, running down the centre of the gel. Squid axoplasm has ripple of similar wave-lengths (*ca.* 5–15 μm, Pl. 3*B*). Remak (1844) pictured ripple-like oscillations in the neurofibrillae of crayfish, but I know of no other studies of such patterns in axoplasm.

Ripple may be made more pronounced by the mechanical abuse of axoplasm, since less ripple is seen in intact axons (after fixation and sectioning), than in extracted axoplasm. It is impossible to see the amount present in live worm axons, but in the more transparent squid axon preparations, dissected with a minimum of bending or stretching, the amount of ripple is also usually small, and may perhaps be attributed to the dissection. Bending or stretching whole squid axons gives more widespread and shorter wave-length ripple patterns, without necessarily affecting the action potential. Extraction of squid axoplasm also results in a more widespread ripple pattern appearing. Regardless of the effects of extraction on ripple amplitude, ripple must nevertheless have some periodic structural basis in axoplasm prior to extraction. One simple hypothesis consistent with these observations is that the neurofilaments are stretched out straight, or nearly so, in axoplasm within the axon, but on extraction they recoil slightly in unison, like released springs, to form a ripple pattern of greater amplitude.

Electron microscopy

Thin sections of *Myxicola* axoplasm show a large array of filaments running down the axon, interrupted only occasionally by a mitochondrion or a vesicle (Pls. 2 and 4). The filaments appear to be morphologically identical throughout the gel, and, when fixed in the conventional manner (i.e. with glutaraldehyde, while inside the ventral cord), the filaments resemble conventional neurofilaments (Pl. 2*A* and *B*; Gilbert *et al.* 1975; and see, for example, Wuerker & Kirkpatrick, 1972). There are 190 ± 50 ($n = 11$) such filaments per square micron of cross-section. Rat sciatic axons have the same number (190 ± 50 per μm^2; calculated from Table 1 of Weiss & Mayr, 1971*a*). When fixed after extraction, however, the filaments appear thinner (diameter near 70–80 Å, Pls. 2*C* and 4), with loosely attached side arms, though the number per square micron of cross-section does not differ significantly. These transitions of *Myxicola* filament morphology have been studied using negative stain techniques, and are discussed in a separate paper (Gilbert *et al.* 1975).

Filament arrangement. When viewed at lower magnifications, the filaments of intact axons do not all lie in a straight array, but instead there are large regions where the filaments commonly swerve in synchonry. The swerving paths appear somewhat sinusoidal in electron micrographs, with periods of roughly 1–12 μm. In extracted axoplasm, this swerving is even more widespread, and amplitudes of the swerving paths are usually larger. In most cases the paths appear consistent with synchronous helical oscillation of the filaments (Pl. 4), if the angle between the plane of section and

the helix axis is taken into account. These are the ripple helices, as seen in thin sections.

More conclusive proof that these oscillations of the filaments are true helices is difficult to acquire for three reasons: (1) the filaments are so tightly intermixed that individual filaments cannot be followed very far; (2) periodicities of the ripple helices are extremely long compared to the filament diameter; so pictures resolving one cannot easily resolve the other; (3) the helices are three-dimensional, requiring many serial sections, exactly in register, for full definition. Twist of the filaments around the central axis of the axon, the segmental helix, is also too gradual to be resolved in electron micrographs.

Composite electron micrographs of large areas of axoplasm show that filaments at least 50 μm apart can swerve in synchrony. This degree of spatial coherence is in accord with the birefringence observations, as are the observed pitches of the ripple helices. Thus both birefringence and electron microscope evidence points to neurofilaments lying in paranemic 'ripple' helices.

Mitochondria and vesicles. These components of *Myxicola* axoplasm are more concentrated near the periphery of both extracted and *in situ* axoplasm, particularly within 1 μm of the edge (Pl. 2). Mitochondria in the giant axon are sinuous cylinders 0·2–0·3 μm in diameter and 1–10 μm in length. They usually lie parallel to the filaments, swerve when the filaments swerve, and often are bent double, like a hair pin (Pl. 2*A*).

The great lengths of the mitochondria make them difficult to count, for one may enter and leave a thin section several times. An estimate of the total amount of mitochondrial material was obtained by measuring, with a light microscope, the mean length and number of mitochondrial fragments in 1 μm thick, serial, longitudinal sections of a short length of extracted axoplasm, 700 μm in diameter. The mitochondrial fragments were on average 3·5 μm long, and their average density was near 6 per 1000 μm^3. The number of fragments within 100 μm of the edge of the axoplasm was 2–3 times the mean density; whereas in the centre of the axoplasm the number fell continuously to $\frac{1}{3}$–$\frac{1}{10}$ the mean density. The fixatives employed gave indications of tubular cristae within the mitochondria, as in squid (Metuzals, 1969), but little additional detail.

Vesicles in the giant axon are spherical (usually 0·1–0·6 μm diameter) and sparse (about 16/100 μm^3) in the interior of the axon (Pl. 4), but irregularly shaped and over ten times as numerous in the periphery (Pl. 2). The great majority appear empty, but a few contain several smaller vesicles within.

Smooth endoplasmic reticulum occurs near the periphery of the axoplasm only, and membranous whorls (Bunge, 1973) are also occasionally found there. These two trace components are rarely evident in extracted axoplasm (Pl. 2*C*).

These amounts of membranous material are consistent with chemical estimates of total lipid in axoplasm (Gilbert, 1975): 6 mitochondrial fragments per 1000 μm^3, each 3·5 μm long and 0·3 μm diameter, corresponds to 0·42 mg mitochondrial lipid per gram of wet axoplasm, given that mitochondria are 25 % lipid by weight (Green & Fleischer, 1964), and have a specific gravity of 1·19 (Marks & Lajtha, 1971). If the mean vesicle density is taken, conservatively, as three times that near the centre of the axon (that is, 50 vesicles per 100 μm^3), and the mean vesicle diameter is 0·3 μm, and if the vesicle membrane contains 3×10^{-7}g lipid/cm^2 (as for frog rod, and red blood cell membranes; Blaurock & Wilkins, 1969; Engelman, 1969), then vesicles in a gram of axoplasm will contain, *in toto*, 0·42 mg lipid. The sum of mitochondrial and vesicle lipid is then 0·84 mg, which compares reasonably well with the 1·24 mg lipid per gram wet axoplasm measured chemically (Gilbert, 1975).

Myxicola axoplasm is a much more homogeneous array of filaments than is squid axoplasm, according to these estimates, since Villegas (1969) shows more vesicles, and quotes mitochondrial densities far higher (30–40 per 100 μm^2) in *Dosidicus gigas* axoplasm than have been found in worm axoplasm. In the squid, *Doryteuthis plei*, mitochondria are estimated to occupy 1 % of the axoplasm volume (Dipolo, 1973), roughly six times more than *Myxicola* contains.

Microtubules. Wells, Besso, Boldosser & Parsons (1972) reported microtubules in electron micrographs of *Myxicola* axoplasm, though Schmitt (1950) found none here. Microtubule-like profiles in my sections have always been resolved into a bundle of neighbouring filaments. Treatment of squid axoplasm in the identical manner showed many, easily resolved microtubules, so the fixation procedure employed here is unlikely to be at fault. Similarly controlled negative stain studies have also shown no microtubules from *Myxicola* axoplasm (Gilbert *et al.* 1975). X-ray data indicate no microtubule component and SDS gel electrophoresis of whole *Myxicola* axoplasm (Gilbert *et al.* 1975) shows very little protein in the position expected for tubulin, the microtubule subunit protein. It seems likely, therefore, that microtubules are, at most, a very minor component of this axoplasm.

Surface contaminants. The surface of extracted axoplasm usually appears free of contaminants in thin sections (Pl. 2*C*). Infrequently, a layer of small vesicles, or a small patch of what appears to be ventral cord tissue lies on the surface. The small mass and sparsity of these contaminants makes them difficult to quantify, though they appear to represent a tiny fraction (probably less than 0·5 %) of the total wet mass.

I do not know where the cleavage between axoplasm and worm occurs during extraction. In both light and electron microscope sections of intact axons, however, there is frequently such a cleavage just inside the membrane (Pl. 2*B*) which suggests that this may be the region of cleavage during extraction as well. Similar cleavage between axoplasm and membrane, in this and other axons, has also been observed at both light microscope (Nicol, 1948*a*; Wells *et al.* 1972), and electron microscope levels (Schlaepfer, 1974).

X-ray diffraction of whole axoplasm

The large quantities of intact *Myxicola* axoplasm available enabled us to obtain the first X-ray diagrams to show evidence of protein structure in axoplasm (Day & Gilbert, 1972). Previous unproductive attempts (Schmitt, Bear & Clark, 1935; Huneeus & Davison, 1970) may fairly be ascribed to the inaccessible, labile and dilute structure of axoplasm. Fresh axoplasm is also more disorderly at the molecular level than, for example, native wool or muscle, since its birefringence is only 1·5 % that of wool (Woods, 1955), and 3 % that of the A band of muscle (Bear *et al.* 1937*a*). Both values are too low to be caused by differences in protein concentrations alone, and so indicate less rigorous alignment of proteins in axoplasm.

Freshly extracted *Myxicola* axoplasm has never yet given discernible X-ray reflexions, despite many attempts, using a wide range of buffers and exposure durations. However, if the axoplasm proteins are concentrated by partially drying the strand, relatively faint α-patterns are consistently obtained. Best results were obtained by drying axoplasm strands under tension, and placing many short lengths of these strands in a parallel bundle in the X-ray beam, at 100 % relative humidity (Pl. 3*C*). The 5 and 10 Å reflexions (Table 1) are characteristic of the ubiquitous keratin-myosin-epidermin-fibrin (K-m-e-f) class of α-proteins (Astbury, 1947), and indicate the presence of coiled α-helical coils (Pauling & Corey, 1953; Crick, 1953) oriented meridionally, i.e. parallel to the long axis of the axoplasm.

TABLE 1. X-ray reflexions of whole *Myxicola* axoplasm (mean ± S.D., $n = 4$)

Meridional	Equatorial
5·2 ± 0·1 Å strong arc	10·2 ± 0·4 Å large diffuse spot
25·6 ± 0·9 Å weak arc	~60 Å strong arc
18·4 ± 0·8 Å very weak arc	4·67 ± 0·07 Å strong arc after stretch ($n = 2$)

Additional meridional arcs near 26 and 18 Å point to a long-range order along the length of the neurofilament, but it is not known whether these arise from two periodicities with these dimensions, or one repeating unit of greater length, of which 18 and 26 Å are submultiples. The 60 Å equatorial arcs probably result from the radial electron-density profile of the neurofilament, sampled by the inter-filament packing function (Fraser & MacRae, 1973). These arcs are unlikely to be due to lipids, since the lipid content of this axoplasm is very low (Gilbert, 1975). No discrete reflexions have been observed at lower angles, indicating the absence of any marked periodicities between 60 and about 800 Å.

Several strategies were tried in order to provide more informative

patterns: the dried sticks of axoplasm were rewetted with various buffers, ranging in pH from 5·6 to 9·0; glutaraldehyde or osmium tetroxide (1 %, w/v, buffered with cacodylate to pH 7·0) were used to fix the proteins before drying; and several electron-dense stains were applied (0·2 M-$AgNO_3$, 0·5 % (w/v) Na phosphotungstate, 1 % (w/v) uranyl acetate) – all with no significant change in the X-ray reflexions. However, weights (10–20 g), used to stretch rewetted coils of axoplasm, did change the diffraction pattern: the α-pattern was replaced by various amounts of the 'β-pattern' (Pl. 3*D*), which is characterized by equatorial arcs near 4·7 Å. This transformation is also characteristic of α-proteins (Fraser & MacRae, 1973), and I found, as expected, that it is accelerated by increased stretch and high temperatures. Meridional reflexions near 1·5 Å and 3·3 Å, though expected in the α and β patterns respectively, have not yet been found.

Squid axoplasm has also provided faint α-patterns. *Loligo forbesi* axoplasm was extruded, homogenized in 20 mM histidine, pH 7·0, and centrifuged for 2 hr at 250,000 *g*. Fibres were pulled from the pellet, and exposed at 100 % relative humidity to the X-ray beam for 2 days. These gave meridional reflexions at 5·1 Å and diffuse equatorial spots centred near 10 Å. The presence of neurofilaments in the sample was verified by electron microscopy. No intact microtubules were detected in these preparations.

The low protein concentration of whole axoplasm, and its apparent lack of long-range periodic structure following the treatments I have used, suggested that purified neurofilament preparations might give more informative diffraction patterns. These have, in fact, been obtained and will be discussed elsewhere (D. S. Gilbert, in preparation).

Regeneration

After undergoing the extraction operation, worms replaced directly into sea water will live indefinitely. Their rapid withdrawal reflexes are gone, but slower movements persist. After 1–2 months, three or more large, parallel axons, about 50 μm diameter, develop where the giant axon was. Electron micrographs reveal a typical web of neurofilaments in these areas. Five out of six worms tested had regained an apparently normal fast withdrawal reflex four months after extraction. When tested electrically, these five gave clear action potentials, which were powerful enough to be recorded with the intact animal lying across four electrodes. Sections of a worm, which gave electrical and behavioural evidence of regeneration, illustrate the reassembly of a giant axon (Pl. 1*D*). There is a pronounced twisting of the handles around the regenerating axon, and little basiphilic stain within it, suggesting that reassembly is like the spinning of a yarn, with neurofilaments from many contributing cell bodies spun together to form the new axon.

Regeneration of the giant axon is contrary to the results of Nicol (1948*b*); however, he looked for regeneration for only 16 days after transecting the entire ventral cord. Regenerated axoplasm is usually impossible to extract, apparently because of its many large branches and handles (Pl. 1 *D*). *Myxicola* are sparsely distributed along the British coast (McIntosh, 1923), so after extraction worms are left in aquaria for a few months to regenerate their giant axons, then replanted where they were found.

II. Bulk properties

Water content, specific gravity, and breaking strength

Water content of *Myxicola* axoplasm is 870 ± 4 g/kg axoplasm ($n = 3$), close to that of *Loligo pealii* (865 ± 5 g/kg, Koechlin, 1955). Fresh axoplasm rose to the surface of solutions containing 15 % or more sucrose by weight, and sank in solutions with 12·5 % or less sucrose. The specific gravity of axoplasm therefore lies between 1·05 and 1·06 g/cm^3 at 20° C (Weast, 1968). The precision of this method is limited by the fact that axoplasm swells more rapidly than it floats or sinks in solutions having 12·5–15 % sucrose.

When pinched, axoplasm markedly resists compression and, when stretched, it shows considerable elasticity. Strands 12 cm long routinely supported 0·25 g weights before drying, during X-ray specimen preparation. While still wet, a typical, 520 μm (unstrained diameter) strand of fresh axoplasm supported up to 3 g before breaking. This corresponds to a breaking strength of about 1·4 kg/cm^2. Strands necked down to a fine point in the region of breakage, and sustained loads of this size for approximately 30 sec.

Though seemingly small, this breaking strength is comparable to that of other α-proteins, if corrected for the large amount of water in axoplasm. Proteins account for only 3·6 % (w/w) of *Myxicola* axoplasm (Gilbert, 1975). This corresponds to 2·8 % (v/v) protein, using the above specific gravity of axoplasm, and assuming the partial specific volume of the proteins is 0·74 (Davison & Taylor, 1960). Therefore the breaking strength of the axoplasm proteins is (1400/0·028), or 50 kg/cm^2, roughly similar to that of Cotswold wool (about 60 kg/cm^2; Crewther, Fraser, Lennox & Lindley, 1965).

Refractive index

Fresh axoplasm placed on the prism of an Abbe refractometer showed two bands: a faint band corresponding to a refractive index of 1·3519 ±

0·0003 ($n=7$); and a darker, but less sharp, band at $1{\cdot}3562 \pm 0{\cdot}0014$. Measurements by reflected light and transmitted light were identical. In all cases the dark band at 1·356 moved slowly to 1·359 or more with time (about 10 min).

When axoplasm was placed on the refractometer prism, some liquid left the gel and spread out a short distance over the prism. The two refractive index values may be interpreted as arising from the gel, and the expressed liquid. The liquid, a thin layer of relatively large surface area, dries more rapidly than the thick gel, giving rise to a dark band of increasingly large and variable refractive index as the liquid dries. The gel can be identified with the faint band (since its surface area is smaller), having a lower and more constant refractive index, 1·3519. This value is probably slightly larger than the refractive index of intact axoplasm, because water loss during extraction and measurement will make the gel more concentrated. The refractive index of a salt and protein solution which mimicked the chemical composition of axoplasm was 1·3510, in reasonable agreement with the above value.

Resistivity

The resistivities of several strands, calculated according to eq. (1), are plotted against their diameters in Text-fig. 4. Resistivity increases with increasing diameter, even when measured at different positions along a single strand. The correlation coefficient for these variables is 0·86, and the probability that they are uncorrelated is less than 0·001. Drying of the strand during measurement increased axoplasm resistance by approximately 1 % min^{-1}. The effect of drying was more marked in smaller diameter strands, as might be expected from the greater ratio of surface to volume. Drying might therefore explain an increased resistivity in smaller diameter gels, but not the opposite relationship shown in Text-fig. 4.

This variation of resistivity with diameter was unexpected, so some effort was made to validate it. For controls, 1 % agar solutions were left to set in glass capillary tubes, then the agar was pushed from the tube and its resistivity was measured by the procedure described above. Resistivities of these gels varied less than 4 Ω cm, and were not dependent on gel diameter. Gels made up with sea water and agar had resistivities of $23{\cdot}3 \pm 2{\cdot}9$ Ω cm, which agrees reasonably well with published values for the resistivity of sea water (20·5 Ω cm, Cole & Hodgkin, 1939). Gels made to mimic axoplasm, with 1 % agar, 300 mM-KCl, and 30 mM-NaCl, had resistivities of $19{\cdot}0 \pm 1{\cdot}0$ Ω cm. For both axoplasm and control gels there was no large (less than 10 %), or systematic change in resistivity with frequency at the three frequencies tested: 0·1, 1, and 10 kHz.

Dependence of resistivity on diameter (as in Text-fig. 4) has not been reported previously. The effect may be real, and may perhaps be related to the radial distribution of retardance (Text-fig. 3). I think it likely, however, that at least part of this effect is caused by slight contamination of axoplasm with a low-resistivity fluid

during extraction. Evidence for such contamination is given below, together with a model which can be used to calculate the resistivity of uncontaminated axoplasm.

During extraction, a small pool (*ca.* 1·0 μl.) of clear fluid, probably serum, collects at the incision, and axoplasm is pulled through this pool on its way out of the worm. Flame photometry of this fluid indicates a Na concentration close to that of sea water, as might be expected for serum from a marine annelid (Prosser & Brown, 1961). A second observation suggesting contamination by extracellular fluids is that extraction, or even movement of axoplasm along a few segments within the axon, leaves the axon inexcitable, presumably because the axon membrane is torn. To estimate the amount of contamination is difficult. I can suggest only an upper limit

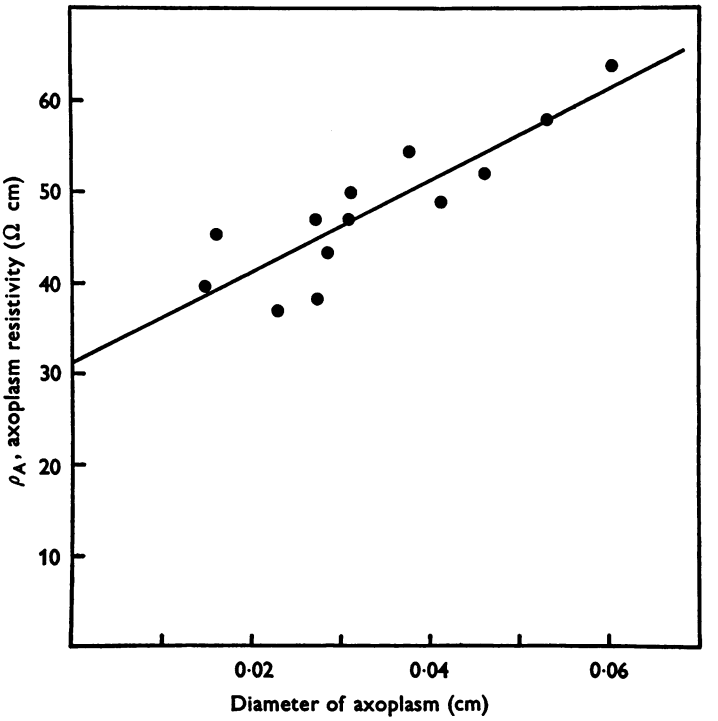

Text-fig. 4. Apparent resistivity of axoplasm, ρ_A, calculated according to eq. (1), plotted against the mean diameter of the strand in the region of measurement. The regression line of resistivity on diameter ($\rho_A = 500D + 31$) is also plotted. Measurements were made at 1 kHz, and 23° C, on nine separate strands. $\rho_A = 48 \pm 8$ Ω cm (mean ± S.D.).

for the average amount: if all contaminating fluids are assumed to have sodium concentrations equal to that of sea water (460 mM) then the average amount of Na in extracted axoplasm (0·34 μmole; Gilbert, 1975) sets an upper limit of 0·34/0·46 = 0·7 mg on the average amount of such contamination on each strand of axoplasm.

The resistivity of uncontaminated axoplasm can be estimated, if three assumptions are made: (1) the contaminant, say 0·7 mg, is uniformly distributed along the length of extracted axoplasm (typically 20 cm); (2) the contaminant has the resistivity of sea water (20 Ω cm) and therefore shunts the axoplasm with a resistance of (20 Ω cm

$\times 20$ cm)/(7×10^{-4}cm^3) = 550 kΩ per cm of axoplasm length; (3) the measured conductance is equal to the sum of the conductances of pure axoplasm and pure contaminant. From these assumptions it follows that the resistivity of pure axoplasm, ρ'_A, can be calculated from:

$$\frac{1}{\rho'_A} = \frac{1}{\rho_A} - \frac{4}{550{,}000\pi D^2},$$

where ρ_A is defined in equation 1, and D is axoplasm diameter. When ρ'_A is calculated for each of the points in Text-fig. 4, the apparent dependence of resistivity on diameter virtually disappears (the correlation coefficient between ρ'_A and D is only 0·02; the regression line is $\rho'_A = 17D + 56$), but the scatter of points increases slightly (ρ'_A mean ± S.D. is 57 ± 9 Ω cm). An alternative assumption, that each strand contains half the maximum average amount of contamination, leads in the same way to somewhat less scattered resistivity values ($\rho'_A = 52 \pm 7$ Ω cm), but higher correlation between ρ'_A and D (correlation coefficient = 0·59; regression line $\rho'_A = 310D + 42$). Closely similar results (with $\rho'_A = 52 \pm 7$ cm) are also given by a different model, in which 0·7 mg of contaminant forms a coat of uniform thickness around the surface of each strand.

From these estimates it appears that the resistivity of *Myxicola* axoplasm lies between 50 and 60 Ω cm, and that its apparent dependence on diameter can plausibly, but not too confidently, be wholly attributed to contamination by extracellular fluids. The data are too scattered to specify an average amount of contaminant, but low correlation between resistivity and diameter requires that the average amount of contaminant be half, or more, of the maximum average amount, 0·7 mg/strand. This point has been considered in detail because it furnishes one of the few available clues for assessing contamination of extracted axoplasm.

Myxicola axoplasm resistivity of 57 ± 9 Ω cm compares favourably with resistivity estimates based on cable theory, for most other axons. These other estimates are (Ω cm): *Sepia*, 63 (Weidmann, 1951); *Carcinus*, 90 (Hodgkin, 1947); frog, 110 (Hodgkin, 1967); and *Eudistylia*, 60 (Hagiwara, Morita & Naka, 1964). Squid axoplasm resistivity is 20–30 Ω cm (Cole & Hodgkin, 1939; Carpenter, Hovey & Bak, 1973); the reason for its low value is unknown. Carpenter *et al.* (1973) also reported preliminary estimates of *Myxicola* axoplasm resistivity of 60–70 Ω cm, in good agreement with the value estimated here.

Diffusion and binding of Na^+, K^+, and homarine

Diffusion estimates require a compromise between high precision and minimum perturbation of the axoplasm. Here the results of three different, simple and direct approaches are described. Each perturbed the axoplasm in a different way, and more than one might wish, but all three yielded similar results.

^{22}Na diffused radially from a strand of axoplasm 970 μm in diameter, and 3·4 cm long, with a time constant of 69 sec. After 6 min the efflux was less than the background noise level. All data fell close to a straight line on a semilog plot (correlation coefficient 0·99), and no detectable ^{22}Na remained

in the axoplasm at the end of the treatment. The radial diffusion coefficient of sodium in axoplasm, calculated from eq. (2), is therefore $5{\cdot}9 \times 10^{-6}$ cm^2 sec^{-1}. This value is 54% of the diffusion coefficient of NaCl in aqueous solution ($1{\cdot}09 \times 10^{-5}$ cm^2 sec^{-1} for 0·2 M-NaCl at 15° C, *Handbook of Chemistry and Physics*, 1947). Only one strand survived the entire treatment intact, but two other strands gave similar data before breaking. Since most improvements in experimental design, such as more rapid stirring in larger volumes, might be expected to increase the measured diffusion coefficient, the agreement between axoplasm and free solution values appears close.

The chief source of uncertainty in this value is that the strand diameter swelled noticeably, then stabilized, during the initial incubation. Swelling was common in all near-physiological buffers, a problem which I have not been able to overcome entirely, short of fixation. To circumvent this problem, longitudinal diffusion of ^{22}Na was measured, since this could be done without immersing the entire strand in buffer.

Longitudinal diffusion coefficients of ^{22}Na were determined in three strands, which gave values of $0{\cdot}7 \times 10^{-5}$, $1{\cdot}4 \times 10^{-5}$ and $1{\cdot}7 \times 10^{-5}$ cm^2 sec^{-1}. Again these lie close to the diffusion coefficient for NaCl in aqueous solution. The chief source of uncertainty in these values is that, over the long time needed to obtain a sufficient flux for counting, axoplasm diameter shrank by up to 30%, even though the axoplasm was inside a sealed container at 100% relative humidity. Axoplasm diameter therefore had to be averaged over time as well as space. Taken together, the radial and longitudinal diffusion data support the hypothesis that Na^+ mobility in axoplasm is isotropic, and similar to that in free solution, since both shrunken and swollen strands give coefficients close to those in free solution.

These measurements may be criticized for their slowness, and for showing that Na^+ *added to* axoplasm, in considerable excess over the native amount, may diffuse freely. They do not show that *native* Na^+ or K^+ has such freedom. To investigate this, effluxes of native Na^+ and K^+ from a pool of five gels were determined by flame photometry, within a few minutes of extraction. Both Na^+ and K^+ effluxes into isosmotic sucrose were found to proceed with time constants of about 200 sec (K^+: 215 sec, correlation coefficient 0·97; Na^+: 240 sec, 0·98), three times longer than that of radial diffusion of ^{22}Na. This discrepancy was attributed to the observed clumping of the strands, and the less effective stirring in the more viscous test solutions. Therefore it appeared that native Na^+ and K^+ diffused, at least qualitatively, much like added ^{22}Na. At the end of this experiment, however, the pool of axoplasm, homogenized in dilute HNO_3, was found to contain about 10 times more Na^+ and K^+ than expected by extrapolation of the efflux curve. This suggested a modicum of bound Na^+ and K^+ was

retained in the axoplasm, even though about 90% diffused freely. The three following experiments were designed to obtain a rough estimate of the proportions of ions retained by the gel framework.

An upper limit for the amount of Na^+ and K^+ bound to the axoplasm was initially estimated by allowing long-term (33 min) equilibration of three strands in a large volume of isosmotic sucrose, with care taken to prevent clumping. At the end of this treatment 6% (14 m-mole/kg axoplasm) of the total amount of native K^+ remained in the axoplasm and 17% (2·5 m-mole/kg axoplasm) of the native Na^+ was similarly retained.

The efflux of native homarine into an EGTA-containing medium, in which the gel swelled less than in the above sucrose solutions, showed qualitatively similar behaviour. Homarine concentration in one strand fell with a time constant of 78 sec, and a correlation coefficient of 0·99; a second, smaller strand gave a time constant of 42 sec. Less than 5% remained in either gel after 5 min. All samples were collected within 6 min of extraction, so this test was the closest in time, and in the buffer environment to the living condition.

Finally, more exact upper limits for the amounts of bound Na^+, K^+ and homarine were estimated by measuring the amounts remaining in three pooled strands after 30 min of stirring in 50 ml. distilled water. Four repetitions of this experiment showed that (56 ± 6)% of the initial Na^+ concentration, (70 ± 6) % of the K^+ and (64 ± 7) % of the homarine left the strands within 3–5 min. The relative amounts remaining in the strands after 30 min, called here 'bound' (though in fact only an upper limit), were $(5{\cdot}4 \pm 1{\cdot}8)$ % of the initial Na^+ concentration, $(2{\cdot}5 \pm 0{\cdot}6)$ % of the K^+, and $(2{\cdot}3 \pm 0{\cdot}9)$ % of the homarine. The pH of the distilled water was $4{\cdot}8 \pm 0{\cdot}1$ before incubation with axoplasm, and $6{\cdot}7 \pm 0{\cdot}5$ afterwards. The pH of stirred controls did not change.

The last data have four interesting aspects. First, as might be expected, less of each component remained bound to axoplasm in water, compared to the amounts bound in the previous, more physiological solutions. Secondly, axoplasm appears to have some buffering capacity and buffers to near pH 7. Thirdly, the proportion of Na^+ leaving axoplasm is consistently less than that of either K^+ or homarine. The 80% slower efflux of Na^+, compared to K^+, in the first 3–5 min fits well with the known 70% lower absolute mobility in aqueous solution of Na^+, compared to K^+ (Conway, 1952). The final ratios of amounts bound, however, are larger than expected on this basis, and suggest an additional factor, i.e. slight preference of the retaining sites within axoplasm for Na^+ rather than potassium. Fourth, over 90% of each of these constituents do not appear, under these test conditions, to be bound to the axoplasm framework. The amounts of cations bound are less than the estimated amounts of acid residues in the

gel proteins (about 60 m-moles/kg axoplasm, though an unknown fraction may occur as amides; Gilbert, 1975). Therefore the amounts of cations bound may be simply accommodated by these fixed charges, without postulating more complex binding schemes.

Myxicola diffusion and binding data agree well with those measured by quite different methods in other axons. The diffusion coefficient of Na^+ radially through squid axoplasm is $(6{\cdot}5 \pm 2{\cdot}0) \times 10^{-6} cm^2 sec^{-1}$ (Hodgkin & Keynes, 1956), compared with $5{\cdot}9 \times 10^{-6} cm^2 sec^{-1}$ for *Myxicola*. Radial andl ongitudinal diffusion coefficients for Na^+ in *Myxicola* do not differ significantly; their mean value is $(11{\cdot}0 \pm 5{\cdot}4) \times 10^{-6} cm^2 sec^{-1}$, close to that $(10{\cdot}9 \times 10^{-6} cm^2 sec^{-1})$ of NaCl in free solution. K^+ diffuses about 1·25 times faster than Na^+ in *Myxicola* axoplasm, therefore K^+ may be expected to have a diffusion coefficient near $14 \times 10^{-6} cm^2 sec^{-1}$, well within experimental error of the $15 \times 10^{-6} cm^2 sec^{-1}$, estimated by Hodgkin & Keynes (1953) for diffusion of K^+ in both *Sepia* axoplasm and in free solution. Hinke (1961), using ion-selective glass electrodes in squid axons, also found that K^+ in axoplasm behaves like that in free solution, but estimated that 24 % of axoplasm Na^+ may be bound. This discrepancy with the 5–17 % measured in *Myxicola* may be caused, in part, by the lower ionic strength solutions used in the *Myxicola* measurements, or by the assumption of 100 % free K^+, used by Hinke.

DISCUSSION

Myxicola axoplasm can be extracted quickly, simply and reproducibly. The yield is approximately 30 mg (wet weight) per worm. Contamination is slight: there are few visible surface contaminants, and less than about 3 % fluid contaminants. Extraction leaves the axon membrane inexcitable; therefore this operation is not a good beginning for axon membrane studies. On the other hand, extraction appears to be a useful technique for study of the axon interior.

Myxicola axoplasm is both a highly hydrated, and a highly structured gel, and so shares many properties of both fluids and solids. Submicroscopic particles, such as ions, diffuse through the gel as if it were an aqueous solution; whereas the gel responds to macroscopic mechanical probes like an elastic solid. In the next two sections, fluid and solid aspects of axoplasm are considered, together with alternative views, in which axoplasm has been interpreted, microscopically, as a solid, or macroscopically, as a fluid.

Is *Myxicola* axoplasm representative of that found in other axons? The few available quantitative data from other axons have been presented with the *Myxicola* results. These indicate that the *Myxicola* axon and other axons have similar values for all of the following parameters: water content, resistivity, birefringence, number of neurofilaments per unit volume, ion diffusion coefficients, and ion binding. There are also many similarities in structure, which are discussed in the second and last sections below.

Despite this extensive agreement, there are major differences. The chief difference is *Myxicola*'s lack of microtubules. Microtubules are often presumed to be structural elements in axons (Wuerker & Kirkpatrick, 1972; Daniels, 1972). This analysis shows that neurofilaments are the only significant structural elements in *Myxicola* axoplasm. It remains to be determined how the structural, and other, tasks are divided between microtubules and neurofilaments in more typical axons, which contain both types of proteins. Historically, Schmitt (1950) found microtubules in squid axoplasm, but none in parallel experiments with *Myxicola*, and concluded that the squid preparation was contaminated with extra-axonal material. I have found Schmitt's observations reproducible, and his inference unlucky, for no other axon has been shown to be so devoid of microtubules as *Myxicola*'s. A second difference is that between the polypeptides of *Myxicola* neurofilaments, and those from squid giant axons and vertebrate brain (Gilbert *et al.* 1975; Davison & Winslow, 1974; Huneeus & Davison, 1970). These differences may, however, be more apparent than real, because neurofilament structure is not well understood even in one species, and because the observed differences may result from the action of proteases on a common structure. More work will be required before this point becomes clear.

The structure of *Myxicola* axoplasm has been described in detail because the three-dimensional structure of axoplasm has received little attention in recent decades, and because this axoplasm appears to serve as a flexible internal skeleton for the axon. The latter idea is contrary to the few current theories of axon structure, which emphasize the formative and supportive roles of the axon membrane, and hydrostatic pressure within the axon (Young, 1944; Weiss, 1964). These theories are discussed in the second section below, and an alternative 'twist' hypothesis, linking molecular and macroscopic forms, is developed in the third and fourth sections below. Several common centro-symmetric features of vertebrate nerve cells, which appear to support the twist hypothesis, are discussed in the last section.

Fluid properties of axoplasm: movement of ions

Less than 3% of the volume of *Myxicola* axoplasm is occupied by its mesh of fibrous proteins, the remainder is filled with an aqueous solution of, primarily, inorganic ions and free amino acids (Gilbert, 1975). Are these particles free to move through the gel, or are they immobilized by the gel framework? At first sight, the solid framework and the many acidic residues attached to it (Gilbert, accompanying paper) might suggest widespread immobilization of ions, as postulated in Ling's 'ice cube', or, 'association-induction' hypothesis of cell interiors (Ling, 1962; Ling, Miller & Ochsenfeld, 1973). However, the measurements here of Na^+, K^+, and homarine diffusion show that only small proportions of these are bound, and otherwise their diffusion coefficients are close to those in free solution. It may be objected that all of the buffers used in these measurements somehow 'melted' the 'ice cube'. This possibility is rendered

unlikely by the resistivity measurements, though their interpretation requires some further explanation.

The measurements of axoplasm resistivity were carried out in air, and so are free from the complicating effects of buffers. They were among the most precise, and the most rapid here, being completed within 1–2 min of extraction. They are also in close agreement with measurements on intact *Myxicola* axons (Carpenter *et al.* 1973), but free from the uncertainties of tip potentials, and tip damage, inherent in the use of micro-electrodes (Gabella & North, 1974). Therefore, of the measurements here, these best reflect the movements of ions in *Myxicola* axoplasm. The *expected* resistivity of axoplasm is calculated below, using the measured free ion concentrations and diffusion coefficients. Both expected and measured resistivity values are shown to be in reasonable agreement; therefore the resistivity measurements lend credence to the diffusion coefficient estimates, which, in turn, indicate that the ions are free to move through axoplasm with nearly the mobility they have in free solution.

Potassium ions are the major conducting species, because of the high concentration, C_K, of non-bound ions (about 270 m-mole/kg axoplasm; Gilbert, 1975), and high diffusion coefficient, D_K, estimated here as $1{\cdot}4 \times 10^{-5}$ cm^2 sec^{-1}. The Einstein relation, $D_K = (RT/ZF)U_K$, may be used to determine the potassium mobility, U_K. Z is the valence of the ion, and R, T and F have their usual significance. The conductance caused by K^+ in axoplasm then equals $C_K U_K F$, here 0·014 mho/cm, or (71 Ω cm)$^{-1}$. For chloride, C_{Cl} is about 23 m-mole/kg axoplasm, though the amount bound is unknown, but probably small, since the activity coefficient is high. D_{Cl} has not been measured, but may be taken as, at most, $1{\cdot}5 \times 10^{-5}$ cm^2/sec, the value for 0·5 M-KCl (Hodgkin & Keynes, 1953). This assumption gives a chloride conductance of $1{\cdot}3 \times 10^{-3}$ mho/cm, or (780 Ω cm)$^{-1}$. Similarly for Na, C_{Na} is about 12 m-mole/kg axoplasm, and D_{Na} is $1{\cdot}1 \times 10^{-5}$ cm^2 sec^{-1}, giving a conductance of $4{\cdot}9 \times 10^{-4}$ mho/cm, or (2000 Ω cm)$^{-1}$.

The divalent ions, Ca and Mg, will contribute negligibly because of their very low concentrations, and probable affinities for the acidic residues on the proteins (Baker, Hodgkin & Ridgway, 1971; Alemà, Calissano, Rusca & Giuditta, 1973). Homarine and the many free aliphatic amino acids in *Myxicola* axoplasm carry little net change at pH 7, the pH of axoplasm, and so will contribute negligibly to the total conductance. The acidic amino acids, cysteic, glutamic and aspartic, will, however, contribute significantly to the total conductance, since they occur in high concentrations, totalling about 200 m-mole/kg axoplasm. I have not measured their diffusion coefficients in axoplasm, nor have I been able to find their diffusion coefficients in aqueous solution, but these last values may probably be taken as about 5×10^{-6} cm^2 sec^{-1}, an estimate based on values for similar molecules given by Cohn & Edsall (1943). If acidic amino acids are not bound, and have the same diffusion coefficients in axoplasm, then their total conductance will be about $3{\cdot}7 \times 10^{-3}$ mho/cm, or (270 Ω cm)$^{-1}$.

These conductance values may be summed to give an estimate of the conductance of whole axoplasm: 0·019 mho/cm, or (51 Ω cm)$^{-1}$. This value is in good agreement with the resistivity estimated from direct measurements, 57 ± 9 Ω cm. Interactions between the mobile charges may be expected to account for at least part of the remaining discrepancy. Therefore the ion concentration, ion diffusion, and ion binding

measurements are consistent with the resistivity measurements, and both sets of data are most simply interpreted as arising from ions diffusing through axoplasm, much as they would through free solution, except for a small percentage of ions which remains bound to the gel framework. The fractions of the total current carried by the individual ions (the transport numbers), based on the foregoing assumptions, are: K^+, 0·72; Na^+, 0·02; Cl^-, 0·07; cysteic acid, 0·11; aspartic acid, 0·07; and glutamic acid, 0·01.

Particles larger than a few hundred Ångstroms will be increasingly hindered in their movements through the neurofilament mesh, judging from the pore sizes seen in electron micrographs. Preliminary measurements of the equivalent pore size of the gel, using whole axoplasm as a chromatographic column (Rodbard & Chrambach, 1970), were strongly dependent on the buffer used, and so this parameter remains unknown. Movement of mitochondria (Pomerat, Hendelman, Raiborn & Massey, 1967) would appear to require considerable distortion of the mesh.

Solid properties of axoplasm: how widepsread?

Axoplasm can be pulled out of nearly all *Myxicola* giant axons. The only exceptions are those in moribund worms, which usually have a viscous fluid axoplasm, and which have consistently shown other signs of ill health, such as flaccidity, loss of colour, and shedding of fan and cuticle. Worms long dead always have fluid axoplasm. Therefore fluid axoplasm seems to be a pathological state in *Myxicola*, and an elastic solid axoplasm, the normal, physiological state. The speed of extraction, and the stability of extracted axoplasm for long periods, argue strongly that the consistency of extracted axoplasm is very close to that *in vivo*.

Several factors lead to the breakdown of neurofilaments, and consequently of the solid gel structure. Two such factors are within easy reach of axoplasm *in vivo*. These are high salt concentrations, and Ca ions. Half molar KCl or NaCl breaks down neurofilaments, and approximately this concentration of NaCl is found in the blood. Ca (1–10 mM) activates proteolytic enzymes within extracted axoplasm; these cleave the neurofilament polypeptides (Gilbert *et al.* 1975). About 10 mM-Ca^{2+} is found in sea water, and presumably also in the blood (Prosser & Brown, 1961). Neither salt nor Ca ions, of course, occur at these concentrations in extracted axoplasm (Gilbert, 1975), but the safety margin is narrow. Therefore the solid gel of axoplasm can be rapidly liquefied by pathological states involving only a small, and passive, redistribution of Ca or salt across the axon membrane, or release of Ca from intracellular stores (Baker & Schlaepfer, 1975).

Is axoplasm in other species an elastic solid? Most data come from the squid giant axon, and agree closely with the *Myxicola* data. Thus other authors have concluded that squid axoplasm is normally an elastic solid

(Bear *et al.* 1937*a*; Hodgkin & Katz, 1949; Chambers & Kao, 1952), and I have found that short lengths can be extracted (p. 261). The same factors, calcium ions and high salt concentrations, liquefy both squid and *Myxicola* axoplasm (Hodgkin & Katz, 1949; Huneeus & Davison, 1970), apparently by analogous mechanisms (Orrego, 1971; Gilbert *et al.* 1975). In my experience, squid axoplasm is sometimes as stiff as *Myxicola*'s, but often is less stiff. The cause of this discrepancy has not been established. A likely explanation is that it arises artifactually, from calcium or salt leakage. Squid axoplasm contains higher concentrations of both Ca and Na than *Myxicola* axoplasm (Gilbert, 1975), perhaps as a result of the much longer dissection required, or the fewer protective sheaths around the squid axon. Over-all degeneration late in the squid life-cycle (Holme, 1974), and injuries during capture or storage may also contribute. The proteolytic enzymes in extruded squid axoplasm are partially activated (Orrego, 1971), whereas those in extracted *Myxicola* axoplasm are not (Gilbert *et al.* 1975).

Vertebrate axoplasm, though more difficult to test, also appears to be an elastic gel, similar to *Myxicola* axoplasm: isolated frog axoplasm exhibits considerable stiffness (de Rényi, 1929; Biondi, Levy & Weiss, 1972), and frog, rat and toad sciatic axoplasm can be pulled from its myelin sheaths (Thornberg & De Robertis, 1956). Electron micrographs show no major differences in either the neurofilaments (Gilbert *et al.* 1975), or their packing density (p. 273), compared to those in *Myxicola*. Ca^{2+} accelerates the break-down of neurofilaments in rat peripheral nerves (Schlaepfer, 1974), and the activity of proteolytic enzymes increases after nerve section (Hallpike & Adams, 1969), suggesting the presence of a Ca^{2+} activated protease in degenerating vertebrate axons, similar to those found in squid and *Myxicola*. Degenerating vertebrate axons have long been known to lose their cylindrical shapes, and to adopt beaded shapes having less surface area (Cajal, 1928; Schlaepfer, 1974), as might be expected if a yarn-like internal skeleton turned to fluid as a result of proteolysis.

Despite the above observations, axoplasm is often treated as a viscous fluid (Bullock & Horridge, 1965; Cragg, 1955; Young, 1934, 1936, 1944; Biondi *et al.* 1972). This view, however, is apparently based on experiments in which calcium is very likely to have entered the axoplasm (e.g. Young, 1936; Biondi *et al.* 1972). Therefore the evidence appears to be consistent with the *Myxicola* results, but this treatment probably applies only to a pathological state.

Two theories of axon growth also require that axoplasm behaves like a viscous fluid, contributing only hydrostatic pressure to the maintenance of axon structure. These are Young's (1944) 'turgor pressure' hypothesis, and Weiss' (1964) 'peristaltic pump' hypothesis (see also Weiss & Hiscoe, 1948, and Biondi *et al.* 1972). As noted above, both draw on observations of axoplasm, apparently in the presence of Ca. Both postulate a viscous fluid axoplasm in order to explain the swelling, and more complex forms, which develop just proximal to a cut or a constriction of an axon. The more complex forms include pronounced coiling, as well as telescoping and

ballooning (Weiss & Hiscoe, 1948). Although these forms bear some resemblance to those of fluid flow, they are closely analogous to the contours of a thread, forced ineptly into the eye of a needle. Therefore a yarn-like, elastic solid axoplasm offers a more simple explanation of these features than does the idea of a pipe, bulging and somehow coiling under pressure from within. 'Axonal flow', the growth of fibrous proteins out of the nerve cell body, need not require hydrostatic pressure or peristalsis within the axon as postulated in these theories. Instead, this growth may be compared to the growth of other α-proteins, such as hair. Both hair and axoplasm grow out from ectodermal cells at roughly comparable rates (*ca.* 1 mm/day). Like hair, axoplasm when blocked will coil, or, since neurofilaments are not as tightly cross-linked as the microfibrils of hair, axoplasm may also fray, or balloon, or telescope. These divergent explanations for morphogenesis in nerve cells have close parallels with the older hydrostatic, and more recent filament-based theories of morphogenesis in amoebae and other cells (Allen, Francis & Zeh, 1971; Huxley, 1973).

Weiss & Mayr (1971*a*) adduce two further observations in support of a fluid axoplasm. First, fluid-like contours of neurofilament bundles are seen in electron micrographs of constricted nerve trunks ('whorls', 'streamlines', and 'eddies', *ibid.* p. 849). Because the contours of rivers and ropes are virtually identical, the observed contours might equally well originate not (as for a river) in the *linear momentum* of flowing particles, but in the observed *linear bonding* of a rope-like elastic solid. Secondly, variation in the number of neurofilaments along the length of an axon (though the number per unit cross-sectional area remained roughly constant), suggested to Weiss and Mayr that (*a*) neurofilaments might be a sort of crystallization artifact, likened to the tungsten fibres which form in a melt of tungsten and UO_2, and therefore that (*b*) neurofilaments served no static, architectural function in the axon. Part (*a*) of this interpretation is not the simplest one consistent with the data and therefore it must fall, with part (*b*), to Occam's razor. It does, however, raise the important problem of just how continuous, in time and space, neurofilaments actually are. The *Myxicola* results indicate that at least groups of neurofilaments are sufficiently continuous to maintain a sturdy structure indefinitely under average intracellular ionic conditions, but their lengths and lifetimes in living axons remain to be determined.

As a first approximation, then, *Myxicola*-like elastic solid axoplasm appears to fit most observations of axoplasm in both vertebrates and invertebrates. Description of axoplasm, macroscopically, as an elastic solid is not intended to rule out, or detract from, the microscopic fluid properties noted in the last section, or possible microscopic transport properties (Ochs, 1972; Huxley, 1973; Bray, 1973), or more complex rheological properties, such as creep, set and memory, which commonly occur in other K-m-e-f protein fibres under high stress (Woods, 1955). Contributions to axon structure by membrane-bound proteins cannot be ruled out, though Pl. 2*B*, and considerations of surface/volume ratios, suggest these will be significant only in the smallest axons (*ca.* 1·0 μm diameter or less). It therefore appears desirable to try to link the molecular and macroscopic forms seen in both squid and *Myxicola* axoplasm, and to apply these to the structure of vertebrate axons. This is done in the following sections.

An hypothesis concerning the origin of axoplasm structure

Myxicola axoplasm contains a hierarchy of helices. The X-ray data show a fundamental protein α-helix of pitch about 5 Å, whose axis is coiled into a larger helix, which, in similar proteins, has a pitch of roughly 180 Å, to form the 'coiled-coil' of Pauling & Corey (1953) and Crick (1953). The coiled-coils are themselves coiled into the much larger ripple helices, of pitch about 10 μm; and these, in turn, when twisted into the interconvertible segmental and gel helices of pitch about 1 mm, form the proteins finally into coiled-coiled-coiled-coils, that is, fourth-order compound helices. There are some indications of two or more additional orders of coiling as well: several α-helical coiled-coils may twist about each other to form either protofilaments (Huneeus & Davison, 1970), or neurofilaments (as suggested in Fig. 1). A few neurofilaments may also twist about each other to form bundles (Pl. 4; Metuzals, 1969; Wuerker & Kirkpatrick, 1972).

The compound helix architecture occurs in both *Myxicola*, a variable-length axon from the central nervous system of an annelid, and in *Loligo*, a fixed-length axon from the peripheral nervous system of a mollusc (Metuzals & Izzard, 1969; Metuzals, 1969; and Pl. 3*B*). This coincidence suggests that other axons may share the same architecture, and that the forces which build it may be both simple and general. Three ways of building the structure are discussed below.

It is possible that each helix is deposited in position as a rigid structure. For example, a single isolated neurofilament, in its unstrained configuration, and if sufficiently long, might show both ripple and segmental helix curvature. In the electron microscope, however, isolated neurofilaments show no such rigidity; they appear to be very flexible, with radii of curvature as small as a few hundred Ångstroms (Huneeus & Davison, 1970; Schmitt, 1950; Gilbert *et al.* 1975). This, together with the observed elastic behaviour of the whole gel, suggests that, *in vivo*, a neurofilament's configuration will depend more on the spatial arrangement of its neighbours, and its cross-links to them, than on its own intrinsic stiffness.

Twist could be imposed on the axon from outside, for example, by the surrounding glial cells. This would account satisfactorily for the segmental and gel helices, but could not easily account for the helices inside the axon, such as the ripple helices, nor could it account for the robust, cylindrical axons found in tissue culture, in the absence of glial or other cellular supports. The axon membrane alone is unlikely to exert these shaping forces, both because of its low protein content, relative to that of the axoplasm, and because most membranes so far studied apparently have little intrinsic stiffness (Singer & Nicolson, 1972).

There is, however, one hypothesis which, if true, would enable any array

of parallel, cross-linked filaments to form a cylindrical structure having all the helical forms found in axoplasm. The hypothesis is simply that the filaments behave like twisted elastic rods. A model, built of twisted elastic tubes (which, for this analysis, are sufficiently like rods, and more easily obtained), and showing both ripple and segmental types of helices, is shown in Pl. 5*A*. Its method of construction is given in the caption. In this model identical twisting of all elements before cross-linking creates the ripple helices, and slight untwisting of all elements after cross-linking creates the segmental helices. Similar, but longer, models show two additional features: a gel-segmental helix interconversion; and that the 'axon' will always be approximately cylindrical, regardless of the initial shape of the array at each end-block (Pl. 5*B*). Thus twisted rod models mimic well the observed morphology, including ripple, segmental, and gel helices. Furthermore, similar models can also mimic fork and handle structure, as well as the observed dependence of segmental helix pitch on axoplasm diameter (Pl. 5*C*; Gilbert, 1972*b*).

The twist hypothesis presents three major questions: (*a*) can neurofilaments behave like elastic rods; (*b*) if so, what forces twist them; and (*c*) how is twist controlled? The answer to the first question is likely to be yes, since even narrower filaments, of double-stranded DNA, may be profitably approximated as elastic rods (see Fuller, 1971, for a discussion of the mechanical and molecular factors involved). A possible mechanism causing neurofilament twist is this: the data indicate α-helices oriented along the lengths of neurofilaments, and many acidic residues in the neurofilament proteins. If the α-helical portions contain many of the acidic residues, then changes of pH, or divalent ion concentration near the α-helices will cause them to contract or expand slightly, creating torques about their long axes, and consequent twist of the neurofilament. X-ray data show α-helices to be susceptible to such distortions (Fraser & MacRae, 1973). Thus the structure alone suggests that some neurofilament twist is probably unavoidable, but reliable information concerning the extent of twist, and its method of control, must await a better understanding of neurofilament chemistry and structure.

Several observations of giant fibre axoplasm support the hypothesis that neurofilaments twist: whole squid axoplasm twists markedly when immersed in uranyl acetate (Metuzals, 1969); strips torn from glutaraldehyde-fixed *Myxicola* axoplasm curl into right-handed helices, but more tightly than their intact configuration permitted; and fresh *Myxicola* axoplasm, when suspended in water, twists slowly so as to unwind its segmental helix. It also undergoes a similar, but more violent, twisting motion when suspended in formamide.

Mechanical characteristics of twisted-filament models

These models (Pl. 5) illustrate one way a cell can build a large, relatively rigid structure from tiny, non-rigid elements. The model structure is a self-twisting yarn, and, like yarn, should maintain a stable 'core conductor' geometry in the face of compressional, flexural or tensile forces anywhere along its length. These properties are especially necessary for the long processes of nerve cells, for which any loss of structural continuity causes often-permanent loss of function. This architectural design has the additional property that torques of the filaments are summed, enabling the array to exert large torques, with, perhaps, macroscopic and controlled consequences.

The configuration that minimizes the stored elastic energy of a single, twisted, elastic rod is a helix. This result was first obtained analytically by Euler (Love, 1927), and is used here for modelling the ripple helix. The only other mechanical behaviour fundamental to the model is that two or more twisted elastic rods, when linked together, will twine around each other ('plectonemic coiling', John & Lewis, 1965), until the stored elastic energy of the array is minimized. A dimensional argument, based on Hooke's Law, indicates that the extent of plectonemic coiling will be greater for arrays with fewer rods (Gilbert, 1972*b*). This suggests that smaller diameter axons will have more twist than larger diameter axons, a result observed in *Myxicola* (Gilbert, 1972*b*). Twist in axons may also serve an important structural role, as it does in yarn: 'Twisting gives a short-fibre yarn its strength by diverting part of any tensile load on it into lateral pressure among the fibres that keeps them from slipping past one another' (Backer, 1972, p. 47).

Three features of these models are not essential. First, cross-links between rods are in one plane (the end-blocks) for convenience only; similar forms arise if cross-links are distributed throughout the volume of the model. Secondly, only a small number of rods have to be twisted before the forms appear; so both twist and cross-links may be distributed in time as well as space. Thirdly, for simplicity I identify one rod in the model with one neurofilament. The putative mechanical unit bearing the torsional couple in axoplasm could be either slightly smaller or larger than this, e.g. a single coiled-coil, or a bundle of a few neurofilaments.

Twisted-filament models are independent of scale, and may be applied, in bootstrap fashion, to successively higher levels of organization. Thus the entire plectonemic coil at one level may be viewed as a single twisted rod component of the next higher level of plectonemic coiling. Although only one level has been considered so far (plectonemic coiling of neurofilaments to form the ripple and segmental helices), several additional observations of axon structure could be simply accommodated in such a hierarchy: At the lowest level, α-helices coil plectonemically to form coiled-coils. Each of these may be regarded as one of the twisted rods which coil plectonemically to form a neurofilament (this step is speculative, since neurofilament structure is insufficiently known). Each neurofilament, as discussed above, may be regarded as one of a set of twisted elastic rods which coil plectonemically to form the axoplasm. Finally, each axon in a nerve trunk may be regarded as a twisted elastic rod, in order to account for the 'Bands of Fontana' (synchronous helices of parallel axons, similar to the 'ripple' in Pl. 5*A*), seen in many living nerve trunks (Clarke & Bearn, 1972).

Quantitative treatment of such a hierarchy of structures presents great difficulties. Even at one level of coiling, twisted filament models are mechanically quite complex, and so have been presented in analog form. However, one simple rule may prevail: for maximum stability, successive levels of plectonomeic coiling should alternate in handedness. Thus all naturally occurring α-helices are right-handed, and, in accord-

ance with this rule, all known coiled-coils are left-handed (Fraser & MacRae, 1973). The number of levels of plectonemic coiling above this, including possible protofilaments, neurofilaments, and neurofilament bundles is not yet sufficiently well established to apply this rule further. The handedness rule confers several sorts of stability: (*a*) it promotes conservation of twist, since untwisting of one level will simultaneously twist neighbouring levels more tightly; (*b*) it minimizes friction and wear of surface fibres if the coil moves, since surface fibres are aligned nearly parallel to the length of the coil; (*c*) it counteracts kink and twisted-loop formation by balancing opposite twists locally. Not only does the rule give stable final forms, it also assists assembly of plectonemic coils in this fashion: Two or more identical strands, if twisted into a plectonemic coil, will each be stretched slightly. If each strand has a helical substructure, then this stretch will cause a torque about the axis of each strand. The torques so produced will either promote further plectonemic coiling (a positive feed-back, self-assembly process), or act to unwind the plectonemic coil. The torque will promote self-assembly only if the alternate-handedness rule is obeyed.

Twisted filaments model may apply to other structures, since somewhat similar helical forms are also seen in collagen fibrils (Bouteille & Pease, 1971), in chomosomes (John & Lewis, 1965), and in the long, cylindrical, and actively twisting pseudopodia of some amoebae (Bovee, 1964), and slime moulds (Kamiya & Seifriz, 1954).

The twist hypothesis, and other nerve cells

A twisted-filament structure might help to explain several heretofore puzzling features of vertebrate nerve cells: Axons and dendrites commonly form corkscrew shapes, like *Myxicola*'s gel helix, especially near cuts or constrictions (Cajal, 1928, p. 647; Young, 1944; Weiss & Hiscoe, 1948). Filaments and microtubules appear, in favourable sections, to spiral within axons and dendrites, as in the segmental helix (Cajal, 1909, vol. 1, p. 458; Peracchia, 1974, fig. 1; Weiss & Mayr, 1971*b*; Wuerker & Kirkpatrick, 1972). Twist of several neurofilaments into a tight bundle would provide a simple mechanism for the condensation of neurofibrils, and help to explain their spiral and ring forms (Young, 1944; Boycott, Gray & Guillery, 1961; Gilbert *et al.* 1975).

Twisted-filament arrays produce torques proportional to the sum of the torques of their component filaments, and, if the latter vary together in time, the array will act like a 'torsional muscle'. If this can occur in axons, such behaviour would explain why many things are found to be wrapped spirally around axons, as though twisted into position by the axon. These things include: glial fibres (Bunge, 1968), myelin lamellae (Geren, 1954; Davison & Peters, 1970), other axons (Robertson, 1962), collateral branches of the same axon (called 'nervous spools' for their similarity to thread wound many times around a spool; Cajal, 1928, p. 217), and dendrites of the same nerve cell (Cajal, 1909, vol. 2, p. 915). Torsional movements of the protein array might also explain why the nuclei of developing nerve cells usually rotate. They rotate once every 1–5 hr

(Pomerat *et al.* 1967), a rate not unlike that of the development of myelin lamellae (Davison & Peters, 1970).

Myelination deserves further comment because it is both medically important and poorly understood. Current theories of myelination suppose that (*a*) in peripheral nerves, an unknown control mechanism causes the *outer* flap of the Schwann cell (containing the nucleus) to move repeatedly around the circumference of a stationary axon, leaving behind a trail of myelin lamellae, and, (*b*) in the central nervous system, where one cell forms dozens of myelin sheaths (so rendering method *a* topologically impossible), the *inner* lip of each myelin sheath, powered and controlled by unknown mechanisms, moves around a stationary axon, leaving a similar trail of myelin (Davison & Peters, 1970). Geren (1954) first suggested that the same final forms could be simply developed by having the axon twist, so wrapping myelin lamellae around itself. This idea was largely abandoned when Robertson (1962), found that myelin sheaths in two neighbouring internodes (along a single axon) could spiral in opposite directions. I suggest that axon twist may nevertheless power myelination of both central and peripheral axons, it being necessary only to suppose that, in the sheaths described by Robertson, one sheath slipped (over either the axon, or the outside environment), while the other was developed. These assumptions, of local twist in either direction by the axon, and of sheath slippage, are more explicit and parsimonious than the two preceding schemes, though all must await the judgement of experiment.

To summarize, the relative homogeneity and bulk of axoplasm, in comparison with other portions of typical nerve cells, offers hope of comprehensive biochemical and physiological understanding. The speed and yield of *Myxicola* axoplasm extraction make it appear a particularly useful first step in such analyses. The data here elucidate the functions of axoplasm as an ion reservoir, and as a flexible, but compression-resistant, internal skeleton. They suggest further that the structural design of this skeleton influences the shapes of nerve cells, and their enveloping sheaths.

The late Trevor I. Shaw first suggested that I look at the *Myxicola* axon in 1967, on a day when squid were not available for experiments. He continued to encourage and advise this work until his untimely death in 1972. Barbara Newby and Brian Anderton have also given continued help and advice. Don Wright assisted with the light microscopy, and Brian Kirkham and John Pacy helped with the electron microscopy. Freda Collier and Zolly Gabor prepared the Plates. J. D. Robertson, F. O. Schmitt, J. Z. Young and P. A. Weiss kindly drew my attention to several useful references. Helpful comments on the manuscript were given by John Scholes, Bill Leib, Dennis Bray, Alan Blaurock and Brian Boycott. The Director and staff of the Marine Biological Laboratory, Plymouth, provided facilities and animals. This work was supported by grants from the USPHS (1F2NB37/74901), S.R.C. (B/RG/14705), and M.R.C.

REFERENCES

ALEMÀ, S., CALISSANO, P., RUSCA, G. & GIUDITTA, A. (1973). Identification of a calcium-binding, brain specific protein in the axoplasm of squid giant axons. *J. Neurochem.* **20**, 681–689.

ALLEN, R. D., FRANCIS, D. & ZEH, R. (1971). Direct test of the positive pressure gradient theory of pseudopod extension and retraction in Amoebae. *Science, N.Y.* **174**, 1237–1240.

ANDERTON, B. H., DAY, W. A., GILBERT, D. S. & NEWBY, B. J. (1974). The protein composition of axoplasm from the giant nerve fibres of *Myxicola infundibulum* and *Loligo forbesi*. *Biochem. Soc. Trans.* **2**, 660–661.

APÁTHY, S. (1897). Das leitende Element des Nervensystems und seine topographischen Bezeihungen zu den Zellen. *Mitt. zool. Stn Neapel* **12**, 495–748.

ASTBURY, W. T. (1947). On the structure of biological fibres and the problem of muscle. *Proc. R. Soc.* B **134**, 303–328.

BACKER, S. (1972). Yarn. *Scient. Amer.* **227**, 47–56.

BAKER, P. F., HODGKIN, A. L. & RIDGWAY, E. B. (1971). Depolarization and calcium entry in squid giant axons. *J. Physiol.* **218**, 709–755.

BAKER, P. F., HODGKIN, A. L. & SHAW, T. I. (1962). Replacement of the axoplasm of giant nerve fibres with artificial solutions. *J. Physiol.* **164**, 330–354.

BAKER, P. F. & SCHLAEPFER, W. (1975). Calcium uptake by axoplasm extruded from giant axons of *Loligo*. *J. Physiol.* **249**, 37–38*P*.

BAYLISS, W. M. (1914). *Principles of General Physiology*. London: Longmans.

BEAR, R. S., SCHMITT, F. O. & YOUNG, J. Z. (1937*a*). The ultrastructure of nerve axoplasm. *Proc. R. Soc.* B **123**, 505–519.

BEAR, R. S., SCHMITT, F. O. & YOUNG, J. Z. (1937*b*). Investigations on the protein constituents of nerve axoplasm. *Proc. R. Soc.* B **123**, 520–529.

BINSTOCK, L. & GOLDMAN, L. (1967). Giant axon of *Myxicola:* Some membrane properties as observed under voltage clamp. *Science, N.Y.* **158**, 1467–1469.

BIONDI, R. J., LEVY, M. J. & WEISS, P. A. (1972). An engineering study of the peristaltic drive of axonal flow. *Proc. natn. Acad. Sci. U.S.A.* **69**, 1732–1736.

BLAUROCK, A. E. & WILKINS, M. H. F. (1969). Structure of frog photo-receptor membranes. *Nature, Lond.* **223**, 906–909.

BORN, M. & WOLF, E. (1964). *Principles of Optics*. London: Pergamon.

BOUTEILLE, M. & PEASE, D. C. (1971). The tridimensional structure of native collagenous fibrils, their proteinaceous filaments. *J. Ultrastruct. Res.* **35**, 314–338.

BOVEE, E. C. (1964). Morphological differences among pseudopodia of various small amoebae and their functional significance. In *Primitive Motile Systems in Cell Biology*, ed. ALLEN, R. D. & KAMIYA, N., pp. 189–219. London: Academic Press.

BOYCOTT, B. B., GRAY, E. G. & GUILLERY, R. W. (1961). Synaptic structure and its alteration with environmental temperature: a study by light and electron microscopy of the central nervous system of lizards. *Proc. R. Soc.* B **154**, 151–172.

BRAY, D. (1973). Model for membrane movements in the neural growth cone. *Nature, Lond.* **244**, 93–96.

BULLOCK, T. H. & HORRIDGE, G. A. (1965). *Structure and Function in the Nervous Systems of Invertebrates*, vol. 1, p. 92. San Francisco: Freeman.

BUNGE, M. B. (1973). Fine structure of nerve fibres and growth cones of isolated sympathetic neurons in culture. *J. cell Biol.* **56**, 713–735.

BUNGE, R. P. (1968). Glial cells and the central myelin sheath. *Physiol. Rev.* **48**, 197–251.

CAJAL, S. R. (1909). *Histologie du Système Nerveux*, vols. 1 and 2. trans. AZOULAY, L. Madrid: Consejo superior de investigaciones cientificas, Instituto Ramón y Cajal, 1952.

CAJAL, S. R. (1928). *Degeneration and Regeneration of the Nervous System*, vols. 1 and 2; trans. by MAY, R. M., New York: Hafner, 1959.

CARPENTER, D. O., HOVEY, M. M., & BAK A. F. (1973). Measurements of intracellular conductivity in *Aplysia* neurones: evidence for organization of water and ions. *Ann. N.Y. Acad. Sci.* **204**, 502-530.

CARSLAW, H. S. & JAEGER, J. C. (1959). *Conduction of Heat in Solids*. Oxford: University Press.

CHAMBERS, R. & KAO, C.-Y. (1952). The effect of electrolytes on the physical state of the nerve axon of the squid and of Stentor, a protozoon. *Expl Cell Res.* **3**, 564–573.

CLARKE, E. & BEARN, J. G. (1972). The spiral nerve bands of Fontana. *Brain* **95**, 1–20.

COHN, E. J. & EDSALL, J. T. (1943). *Proteins, Amino Acids and Peptides*. New York: Reinhold.

COLE, K. S. & HODGKIN, A. L. (1939). Membrane and protoplasm resistance in the squid giant axon. *J. gen. Physiol.* **22**, 671–687.

CONWAY, B. E. (1952). *Electrochemical Data*. Amsterdam: Elsevier.

CRAGG, B. G. (1955). A physical theory of the growth of axons. *J. cell. comp. Physiol.* **45**, 33–59.

CREWTHER, W. G., FRASER, R. D. B., LENNOX, F. G. & LINDLEY, H. (1965). The chemistry of keratins. *Adv. Protein Chem.* **20**, 191–346.

CRICK, F. H. C. (1953). The packing of α-helices: simple coiled coils. *Acta crystallogr.* **6**, 689–697.

DANIELS, M. P. (1972). Colchicine inhibition of nerve fiber formation *in vitro*. *J. cell Biol.* **53**, 164–176.

DAVISON, A. N. & PETERS, A. (1970). *Myelination*. Springfield, Illinois: Thomas.

DAVISON, P. F. & TAYLOR, E. W. (1960). Physical-chemical studies of proteins of squid nerve axoplasm, with special reference to the axon fibrous protein. *J. gen. Physiol.* **43**, 801–823.

DAVISON, P. F. & WINSLOW, B. (1974). The protein subunit of calf brain neurofilament. *J. Neurobiol.* **5**, 119–133.

DAY, W. A. & GILBERT, D. S. (1972). X-ray diffraction pattern of axoplasm. *Biochim. biophys. Acta* **285**, 503–506.

DE RÉNYI, G. ST (1929). The structure of cells in tissues as revealed by microdissection. *J. comp. Neurol.* **47**, 405–425.

DIPOLO, R. (1973). Calcium efflux from internally dialyzed squid giant axons. *J. gen. Physiol.* **62**, 575–589.

ELLIOTT, A. (1965). The use of toroidal reflecting surfaces in X-ray diffraction cameras. *J. scient. Instrum.* **42**, 312–316.

ENGELMAN, D. M. (1969). Surface area per lipid molecule in the intact membrane of the human red cell. *Nature, Lond.* **223**, 1279–1280.

FRANKS, A. (1955). An optically focusing X-ray diffraction camera. *Proc. phys. Soc.* **68**, 1054–1064.

FRASER, R. D. B. & MACRAE, T. P. (1973). *Conformation in Fibrous Proteins*. New York: Academic Press.

FULLER, F. B. (1971). The writhing number of a space curve. *Proc. natn. Acad. Sci. U.S.A.* **68**, 815–819.

GABELLA, G. & NORTH, R. A. (1974). Intracellular recording and electron microscopy of the same myenteric plexus neurone. *J. Physiol.* **240**, 28–30*P*.

GEREN, B. B. (1954). The formation of the schwann cell surface of myelin in the peripheral nerves of chick embryos. *Expl Cell Res.* **7**, 558–562.

GILBERT, D. S. (1972*a*). Helical structure of axoplasm. *J. Physiol.* **222**, 44–45*P*.

GILBERT, D. S. (1972*b*). Helical structure of *Myxicola* axoplasm. *Nature, New Biol.* **237**, 195–198.

GILBERT, D. S. (1973). Mechanical models of axon structure. *J. Physiol.* **229**, 3–5*P*.

GILBERT, D. S. (1975). Axoplasm chemical composition in *Myxicola* and solubility properties of its structural proteins. *J. Physiol.* **253**, 303–319.

GILBERT, D. S., NEWBY B. & ANDERTON, B. (1975). Neurofilament disguise, destruction and discipline. *Nature, Lond.* **256**, 586–589.

GILBERT, D. S. & SHAW, T. I. (1969). Extrusion and perfusion of the giant nerve fibre of *Myxicola infundibulum*. *J. Physiol.* **204**, 28–29*P*.

GOLDMAN, L. & SCHAUF, C. L. (1972). Inactivation of the sodium current in *Myxicola* giant axons. *J. gen. Physiol.* **59**, 659–675.

GREEN, D. E. & FLEISCHER, S. (1964). Role of lipid in mitochondrial function. In *Metabolism and Physiological Significance of Lipids*, ed. DAWSON, R. M. C. & RHODES, D. M. London: Wiley.

HAGIWARA, S., MORITA, H. & NAKA, K. (1964). Transmission through distributed synapses between two giant axons of a sabellid worm. *Comp. biochem. physiol.* **13**, 453–460.

HALLPIKE, J. F. & ADAMS, C. W. M. (1969). Proteolysis and myelin breakdown: a review of recent histochemical and biochemical studies. *Histochem. J.* **1**, 559–578.

Handbook of Chemistry and Physics (1947), vol. 30. Cleveland, Ohio: Chemical Rubber Publishing Company.

HINKE, J. A. M. (1961). The measurement of sodium and potassium activities in the squid axon by means of cation-selective glass micro-electrodes. *J. Physiol.* **156**, 314–335.

HODGKIN, A. L. (1947). The membrane resistance of a non-medullated nerve fibre. *J. Physiol.* **106**, 305–318.

HODGKIN, A. L. (1967). *The Conduction of the Nervous Impulse*. Liverpool: University Press.

HODGKIN, A. L. & KATZ, B. (1949). The effect of calcium on the axoplasm of giant nerve fibres. *J. exp. Biol.* **26**, 292–294.

HODGKIN, A. L. & KEYNES, R. D. (1953). The mobility and diffusion coefficient of potassium in giant axons from *Sepia*. *J. Physiol.* **119**, 513–528.

HODGKIN, A. L. & KEYNES, R. D. (1956). Experiments on the injection of substances into squid giant axons by means of a microsyringe. *J. Physiol.* **131**, 592–616.

HOLME, N. A. (1974). The biology of *Loligo forbesi* Steenstrup (Mollusca: Cephalopoda) in the Plymouth area. *J. mar. biol. Ass. U.K.* **54**, 481–503.

HUNEEUS, F. C. & DAVISON, P. F. (1970). Fibrillar proteins from squid axons. I. Neurofilament protein. *J. molec. Biol.* **52**, 415–428.

HUXLEY, H. E. (1973). Muscular contraction and cell motility. *Nature, Lond.* **243**, 445–449.

JOHN, B. & LEWIS, K. R. (1965). The meiotic system. *Protoplasmatologia* **6**, 223–242.

KAMIYA, H. & SEIFRIZ, W. (1954). Torsion in a protoplasmic thread. *Expl Cell Res.* **6**, 1–16.

KOECHLIN, B. A. (1955). On the chemical composition of axoplasm of squid giant nerve fibres with particular reference to its ion pattern. *J. biophys. biochem. Cytol.* **1**, 511–529.

KOLTZOFF, N. K. (1906). Studien über die Gestalt der Zelle. *Arch. mikros. Anat. EntwMech.* **67**, 364–572.

LING, G. N. (1962). *A Physical Theory of the Living State*. New York: Blaisdell.

LING, G. N., MILLER, C. & OCHSENFELD, M. M. (1973). The physical state of solutes and water in living cells according to the association-induction hypothesis. *Ann. N.Y. Acad. Sci.* **204**, 6–50.

LOVE, A. E. H. (1927). *A Treatise on the Mathematical Theory of Elasticity*, 4th edn., p. 414. New York: Dover.

McIntosh, W. C. (1923). *The British Marine Annelids*, vol. 4, part 2, Ray Society Monographs. London: Dulau and Co.

Marks, N. & Lajtha, A. (1971). Protein and polypeptide breakdown. In *Handbook of Neurochemistry*, vol. 5, ed. Lajtha, A. London: Plenum.

Metuzals, J. (1969). Configuration of a filamentous network in the axoplasm of the squid (*Loligo pealii*) giant nerve fibre. *J. cell Biol.* **43**, 480–505.

Metuzals, J. & Izzard, C. S. (1969). Spatial patterns of threadlike elements in the axoplasm of the giant nerve fibre of the squid (*Loligo pealii* L.) as disclosed by differential interference microscopy and by electron microscopy. *J. cell Biol.* **43**, 456–479.

Nicol, J. A. C. (1948*a*). The giant nerve fibres in the central nervous system of *Myxicola* (Polychaeta, Sabellidae). *Q. Jl Microsc. Sci.* **89**, 1–45.

Nicol, J. A. C. (1948*b*). The function of the giant axon of *Myxicola infundibulum* Montagu. *Can. J. Res.* **26**, 212–222.

Ochs, S. (1972). Fast transport of materials in mammalian nerve fibres. *Science, N.Y.* **176**, 252–260.

Orrego, F. (1971). Protein degradation in squid giant axons. *J. Neurochem.* **18**, 2249–2254.

Parker, G. H. (1929). The neurofibril hypothesis. *Q. rev. Biol.* **4**, 155–178.

Pauling, L. & Corey, R. B. (1953). Compound helical configurations of polypeptide chains: structure of proteins of the α-keratin type. *Nature, Lond.* **171**, 59–61.

Peracchia, C. (1974). Excitable membrane ultrastructure. 1. Freeze fracture of crayfish axons. *J. cell Biol.* **61**, 107–122.

Pomerat, C. M., Hendelman, W. J., Raiborn, C. W. & Massey, J. F. (1967). Dynamic activities of nervous tissue *in vitro*. In *The Neuron*, ed. Hydén, H. Amsterdam: Elsevier.

Poo, M. & Cone, R. A. (1974). Lateral diffusion of rhodopsin in the photoreceptor membrane. *Nature, Lond.* **247**, 438–441.

Prosser, C. L. & Brown, F. A. (1961). *Comparative Animal Physiology*, 2nd edn., p. 62. London: Saunders.

Remak, R. (1843). Ueber den Inhalt der Nervenprimitivröhren. *Arch. Anat. Physiol. wiss. Med.* pp. 197–201.

Remak, R. (1844). Neurologische Erläuterungen. *Arch. Anat. Physiol. wiss. Med.* pp. 463–472.

Reynolds, E. S. (1963). The use of lead citrate at high pH as an electron-opaque stain on electron microscopy. *J. cell Biol.* **17**, 208–212.

Roberts, M. B. V. (1962). The rapid response of *Myxicola infundibulum* (Grübe). *J. mar. biol. Ass. U.K.* **42**, 527–539.

Robertson, J. D. (1962). The unit membrane of cells and mechanisms of myelin formation. In *Proccedings of the Association for Research in Nervous and Mental Disease*, vol. 40, pp. 94–158. Baltimore: Williams and Wilkins.

Rodbard, D. & Chrambach, A. (1970). Unified theory for gel electrophoresis and gel filtration. *Proc. natn. Acad. Sci. U.S.A.* **65**, 970–977.

Schlaepfer, W. W. (1974). Calcium-induced degeneration of axoplasm in isolated segments of rat peripheral nerve. *Brain Res.* **69**, 203–215.

Schmitt, F. O. (1950). The structure of the axon filaments of the giant nerve fibres of *Loligo* and *Myxicola*. *J. exp. Zool.* **113**, 499–512.

Schmitt, F. O., Bear, R. S. & Clark, G. L. (1935). X-ray diffraction studies on nerve. *Radiology* **25**, 131–151.

Schultz, M. (1871). Allgemeines über die Structurelemente des Nervensystems. In *Handbuch der Lehre von den Geweben*, ed. Stricker, S., pp. 108–136. Leipzig.

Shelanski, M. L., Albert, S., De Vries, G. H. & Norton, W. T. (1971). Isolation of filaments from brain. *Science, N.Y.* **174**, 1242–1245.

SHURCLIFF, W. A. & BALLARD, S. S. (1964). *Polarized Light.* London: van Nostrand.
SINGER, S. J. & NICOLSON, G. L. (1972). The fluid mosaic model of the structure of cell membranes. *Science, N.Y.* **175**, 720–731.
THORNBERG, W. & DE ROBERTIS, E. (1956). Polarization and electron microscope study of frog nerve axoplasm. *J. biophys. biochem. Cytol.* **2**, 475-482.
VON LENHOSSÉK, M. (1910). Über die physiologische Bedeutung der Neurofibrillen. *Anat. Anz.* **36**, 257–281.
VILLEGAS, G. M. (1969). Electron microscope study of the giant nerve fiber of the giant squid, *Dosidicus gigas. J. Ultrastruct. Res.* **26**, 501–514.
WEAST, R. C. (1968) (ed.). *Handbook of Chemistry and Physics.* Cleveland: The Chemical Rubber Publishing Co.
WEIDMANN, S. (1951). Electrical characteristics of *Sepia* axons. *J. Physiol.* **114**, 372–381.
WEISS, P. A. (1964). The dynamics of the membrane-bound incompressible body: A mechanism of cellular and sub-cellular motility. *Proc. natn. Acad. Sci. U.S.A.* **52**, 1024–1029.
WEISS, P. & HISCOE, H. B. (1948). Experiments on the mechanism of nerve growth. *J. exp. Zool.* **107**, 315–395.
WEISS, P. A. & MAYR, R. (1971*a*). Organelles in neuroplasmic ('Axonal') flow: neurofilaments. *Proc. natn. acad. Sci. U.S.A.* **68**, 846–850.
WEISS, P. A. & MAYR, R. (1971*b*). Neuronal organelles in neuroplasmic ('Axonal') flow. II. Neurotubules. *Acta Neuropath.* suppl. 5, 198–206.
WELLS, J., BESSO, J. A., BOLDOSSER, W. G. & PARSONS, R. L. (1972). The fine structure of the nerve cord of *Myxicola infundibulum* (Annelida, polychaeta). *Z. Zellforsch. mikrosk. Anat.* **131**, 141–148.
WOODS, H. J. (1955). *Physics of Fibres.* London: Institute of Physics.
WUERKER, R. B. & KIRKPATRICK, J. B. (1972). Neuronal microtubules, neurofilaments and microfilaments. *Int. rev. Cytol.* **33**, 45–75.
YOUNG, J. Z. (1934). Structure of nerve fibres in *Sepia. J. Physiol.* **83**, 27*P*.
YOUNG, J. Z. (1936). The structure of nerve fibres in cephalopods and crustacea. *Proc. R. Soc.* B **121**, 319–337.
YOUNG, J. Z. (1939). Fused neurons and synaptic contacts in the giant nerve fibres of cephalopods. *Phil. Trans. R. Soc.* **229**, 465–503.
YOUNG, J. Z. (1944). Contraction, turgor and the cytoskeleton of nerve fibres. *Nature, Lond.* **153**, 333–335.

EXPLANATION OF PLATES

PLATE 1

The giant axon of *Myxicola*, *A*, before, *B*, during, and, *C*, after extraction of axoplasm. *D* shows a regenerated axon. *A*, *C* and *D* are light micrographs of transverse sections of the worm ventral cord (VC), and surrounding musculature (M). BV, blood vessel.

A, the giant axon (Ax) normally fills the dorsal portion of the ventral cord, and connects to the muscles through paired ventro-lateral nerve trunks (T).

B, extraction of axoplasm, as described in Methods.

C, just after extraction, virtually all the giant axoplasm is removed, leaving a small, apparently fluid-filled gap (G).

D, about 4 months after extraction, an axon of almost normal size has regenerated. Many large, intensely basiphilic cells along the length of the cord appear to contribute material to the regenerating axon through large, tributary branches (B), and

a central ribbon (R), which lose their basiphilic stain as they merge, in later sections, into the new giant axon. Many handles (H), some quite large, twist around regenerated axons.

PLATE 2

Electron micrographs of *Myxicola* axoplasm, inside the ventral cord (*A*), also inside the ventral cord, but apparently tearing away from the axon membrane (*B*), and *C*, after extraction from the worm.

A, transverse section showing the giant axon's neurofilaments (*nf*) nearly end-on, a mitochondrion (*mit*), the giant axon membrane (*mem*), and surrounding glial cells (*gl*).

B, cleavage between axoplasm and axon membrane, in a section otherwise similar to that in *A*. Gaps like this, but up to a few microns wide, frequently occur in both light and electron microscope specimens. This suggests that cleavage also occurs just inside the membrane during extraction.

C, the edge of extracted axoplasm in an oblique section. The surface has no enveloping membrane, and few visible contaminants. Mitochondria are overexposed to show the swerving paths of the filaments. Apparent filament diameter 85 ± 28 Å, range 45–110 Å.

PLATE 3

Birefringence patterns (ripple) in *A*, *Myxicola* and *B*, *Loligo forbesi*. *C* and *D* are *Myxicola* X-ray patterns showing α and β conformations.

A, a thick, longitudinal section of extracted *Myxicola* axoplasm, fixed and embedded as for electron microscopy, showing the variation in ripple wave-length across the diameter (vertical) of the gel. Polarizer, vertical; analyser, horizontal in both *a* and *b*.

B, extracted, whole squid axoplasm, in 0·5 M-EDTA, pH 7·0, showing a somewhat similar ripple pattern.

C, α-pattern of *Myxicola* axoplasm (oriented vertically) obtained in a 49 hr exposure on a toroid X-ray camera, in vacuum. Fresh axoplasm was rinsed with 0·5 M-EDTA, pH 7, then with water, and stretched, dried and packaged as described in Methods. An equal volume of water was added to the specimen before the exposure. The intense 5·2 Å meridional arcs, and diffuse 10 Å equatorial spots, indicate α-helical coiled-coils oriented vertically. Weak meridional arcs near 26 Å and 18 Å are also visible on the original.

D, a mixture of α and β patterns obtained from a specimen similar to that in *C*, but stretched with a 10 g weight before the exposure. The 5·2 Å arcs decrease in intensity, and equatorial arcs near 4·7 Å appear. Specimen (vertical) in a toroid camera; exposed 46 hr, in a helium atmosphere.

PLATE 4

Synchronous swerving of filaments in a longitudinal section of extracted *Myxicola* axoplasm. The long axis of the axon is approximately vertical. Transverse and longitudinal views of the filaments alternate, as does filament direction, in a way that suggests the filaments are oriented in parallel, synchronous helices, aligned vertically with pitch about 8 μm.

PLATE 5

A, model of axoplasm built of twisted tubes. Initially all tubes were of equal length, not twisted, and ran in parallel directly from end-block to end-block. Each tube was then twisted through two revolutions in the same direction, and plugged

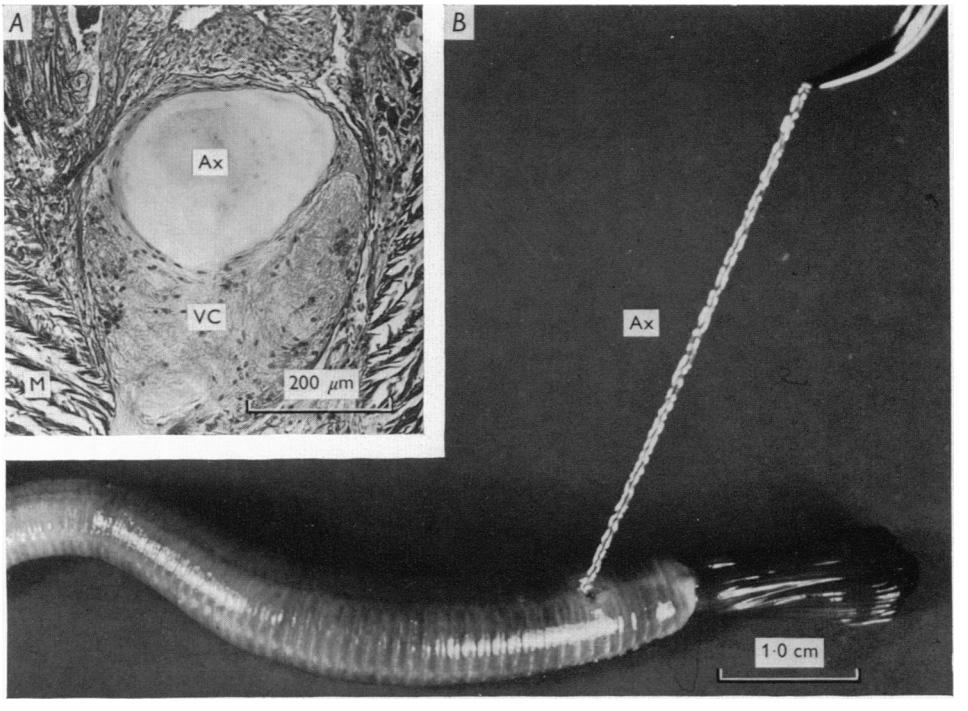

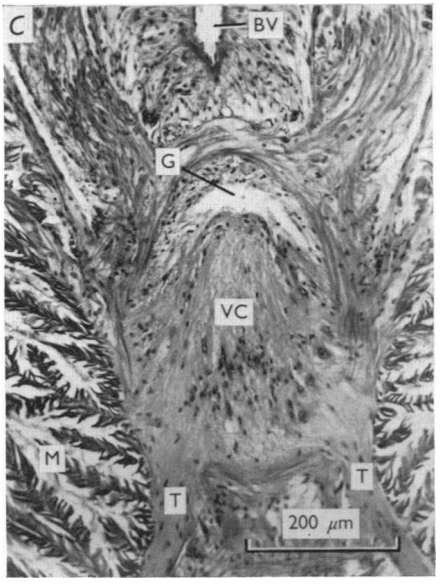

(*Facing p.* 300)

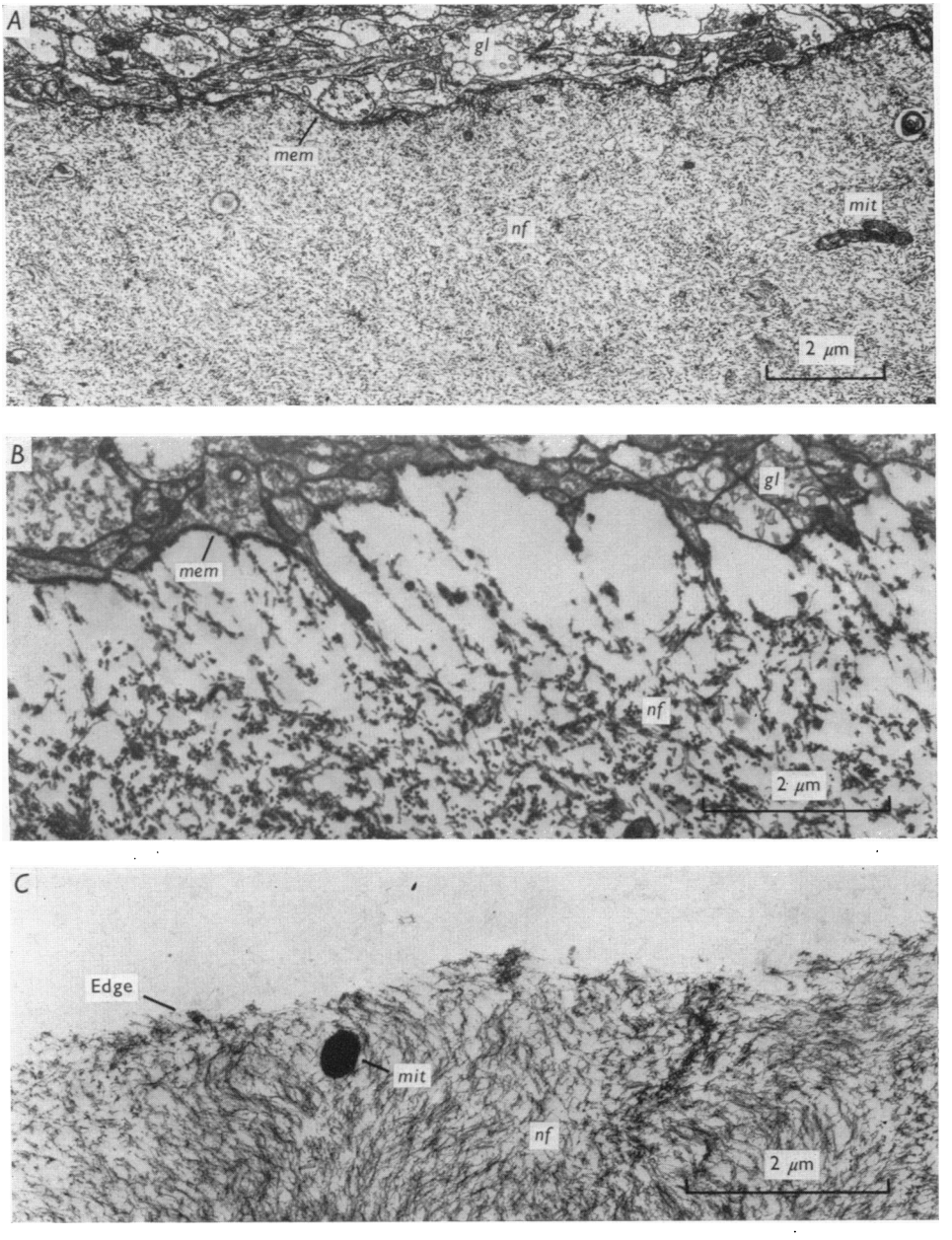
A
gl
mem
nf
mit
2 μm
B
gl
mem
nf
2 μm
C
Edge
mit
nf
2 μm

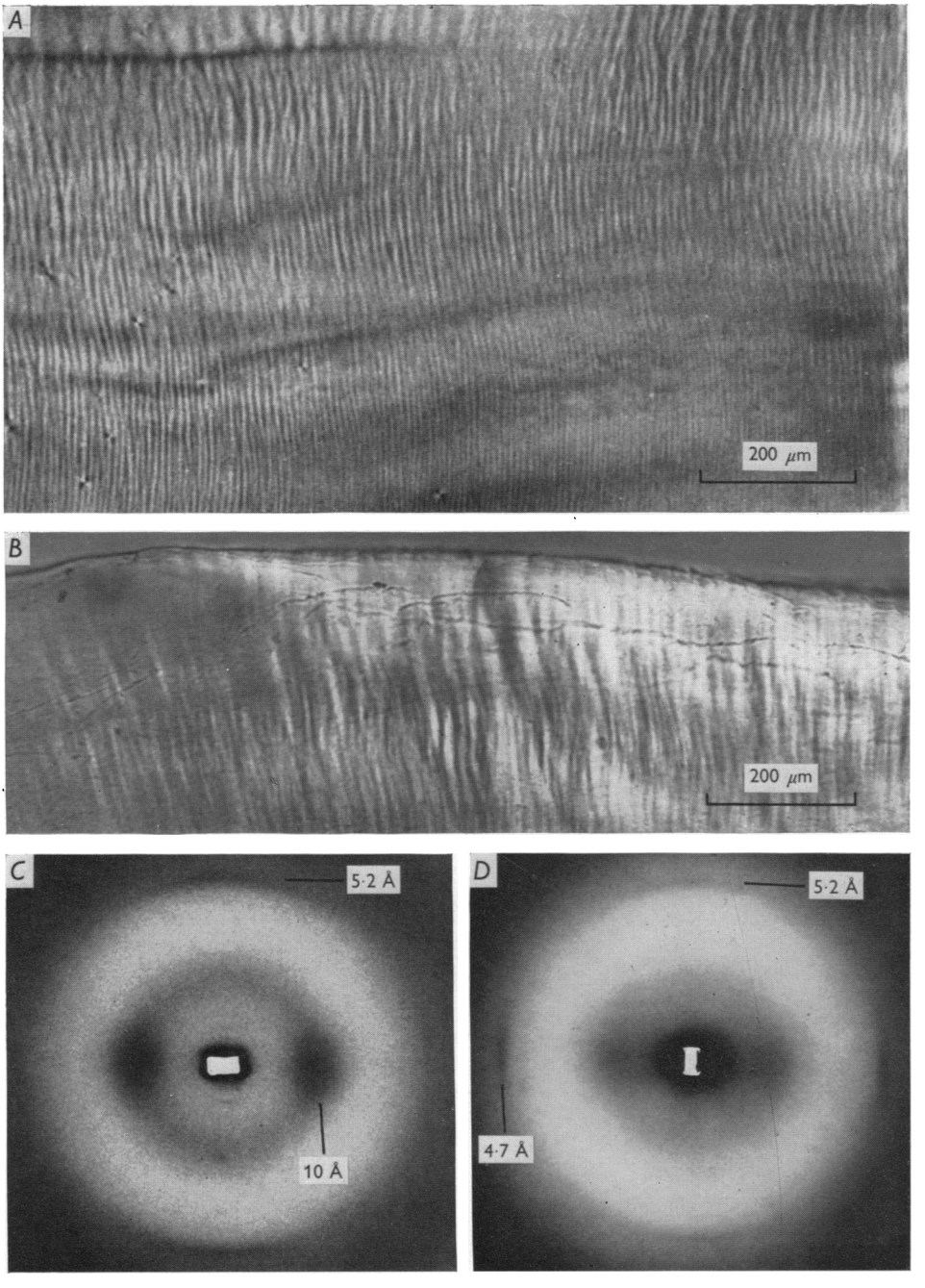

D. S. GILBERT

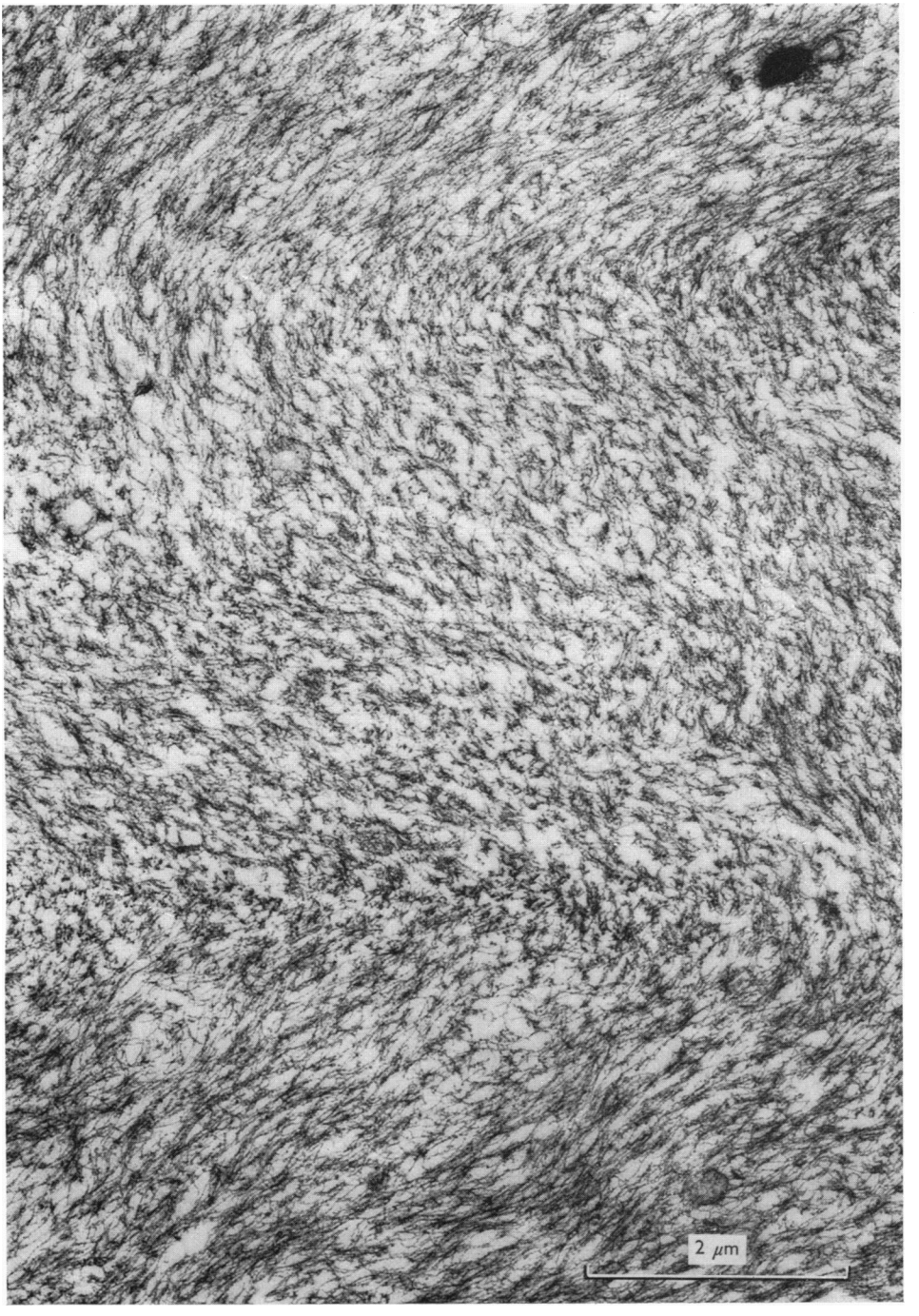
2 μm

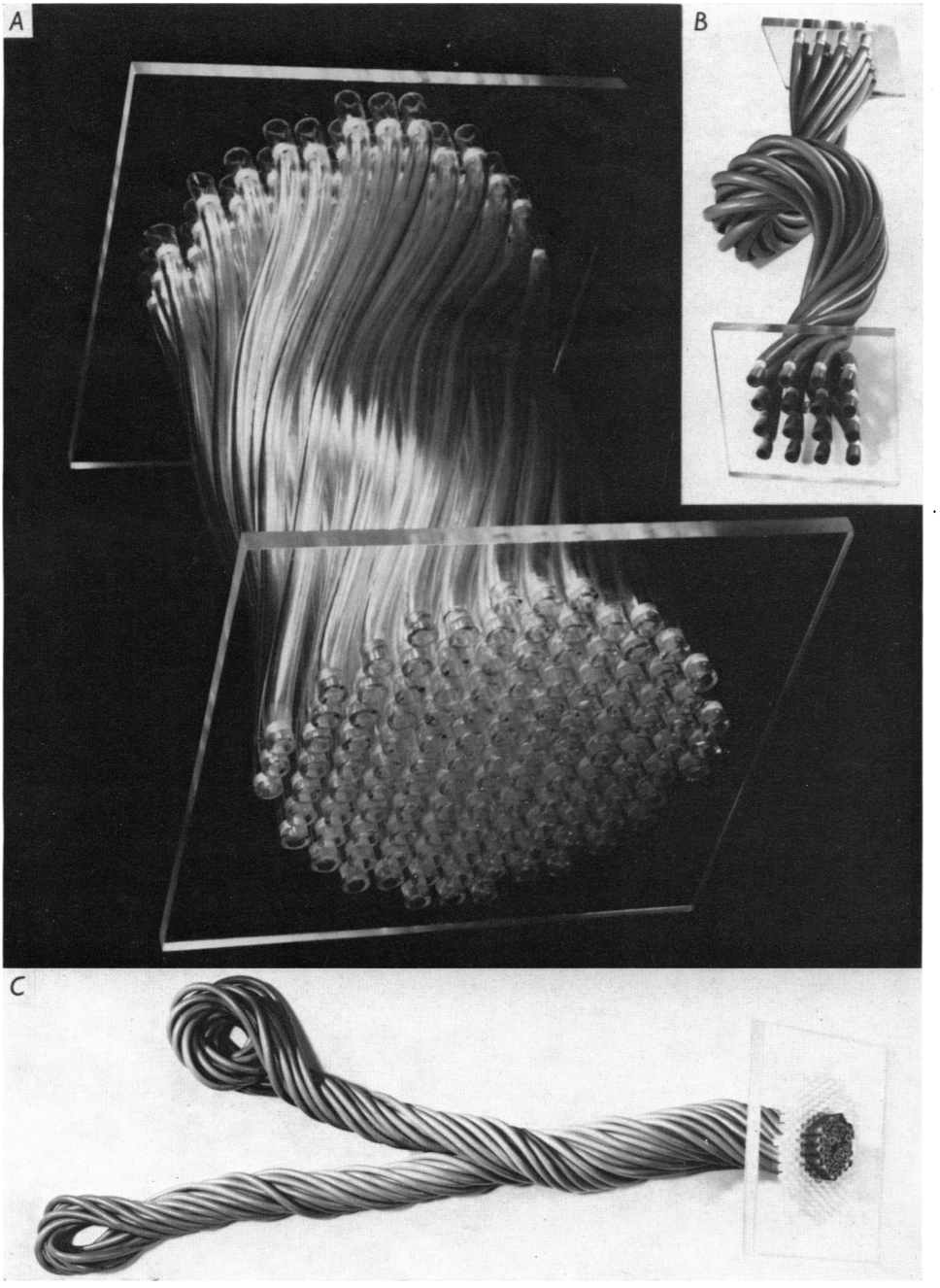

D. S. GILBERT

firmly back into the end block. This twisting had two effects: first, each tube coiled into a helix, identified here with the ripple helix of axoplasm, and visible as a slight undulation of the peripheral tubes. Secondly, the entire array twisted through about 90°, under the combined torques of the individual tubes, until an equilibrium configuration was reached. This overall twist of the array, analogous to the segmental helix twist of axoplasm, compresses the array, and so insures that the ripple helices are tightly and synchronously packed. As in axoplasm, the peripheral elements have the least ripple, because they are the most stretched by twist of the array. Smaller diameter axons have more segmental helix twist, but ripple pitch remains roughly constant near 10 μm (Gilbert, 1972*b*), so this model corresponds to an axon about 10 μm diameter, because its diameter is nearly equal to its ripple pitch.

B, model of the gel helix of axoplasm (partially extended and not to scale), built like that in *A*, but each tube is twisted through four revolutions. This twist causes both the centre line of the array to form one gyre of the gel helix, and each tube to coil about the centre line, as in the segmental helix. This array also forms other stable configurations, since more gel helix coils may be added at the expense of segmental helix twist, and vice versa. Ripple is virtually absent in this array because, unlike *A*, the relatively few (and not highly twisted) tubes allow the twist of each tube to be preferentially absorbed into the segmental helix form.

C, model of a branching axon, terminating in neurofilament rings, and again shaped by equal twists of all tubes. The branch structure is approximately that found by dissection of *Myxicola*'s anterior fork. The ring structure (top left) resembles those found *in vivo* (Boycott *et al.* 1961), and *in vitro* (Gilbert *et al.* 1975).